Development of TiN KID arrays for submm/far-IR astronomy

Jonas Zmuidzinas
+ CIT/JPL KID group

1999 – 2013: MKID (Microwave Kinetic Inductance Detector)

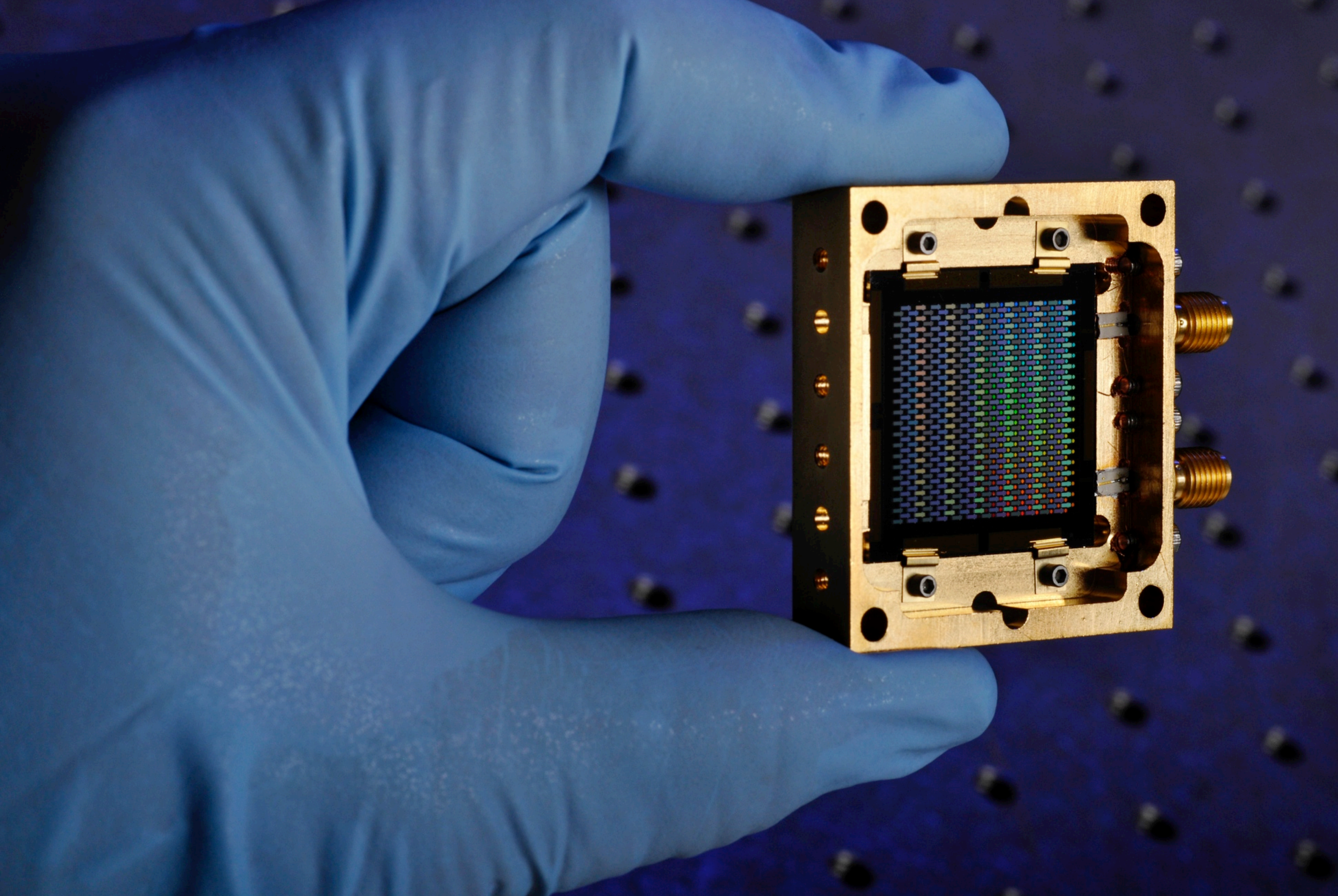

KID/MKID projects

CCAT

INSTITUTIONS	PROJECT	DESCRIPTION
MPIfR Bonn, SRON, TU Delft	A-MKID	20 kpixel submm camera for APEX (R. Gusten)
IRAM, Neel Institute, Cardiff	NIKA2	5 kpixel mm camera for IRAM 30m (A. Monfardini)
UCSB, JPL	ARCONS	2 kpixel optical camera for Palomar (B. Mazin)
Penn, NIST	BLAST upgrade	1000 pixel, dual-pol focal plane for balloon-borne far-IR polarimetry. PI: M. Devlin
Cardiff, SRON, TU Delft, Neel Institute Grenoble, Centro de Astrobiologia (Spain), AimValley, QMC Instruments	spaceKIDS http://www.spacekids.eu/	EU FP7 project. Development of MKID arrays for space applications. PI: Matt Griffin
Argonne National Lab	http://www.aps.anl.gov	Detectors for use with ALS synchrotron
Fermilab	http://www.fnal.gov	100 kpixel optical MKID camera for Dark Energy
NAOJ, U. Tokyo, U. Tsukuba, U. Saitama	http://atc.mtk.nao.ac.jp	CMB polarimetry: GroundBIRD, LITEBIRD
Columbia U.	*SKIP* *http://arxiv.org/abs/1308.0235*	*Balloon-borne CMB polarimetry. PI: A. Miller*
Penn, JPL	*ICarIS*	*Balloon-borne far-IR spectroscopy. PI: J. Aguirre*

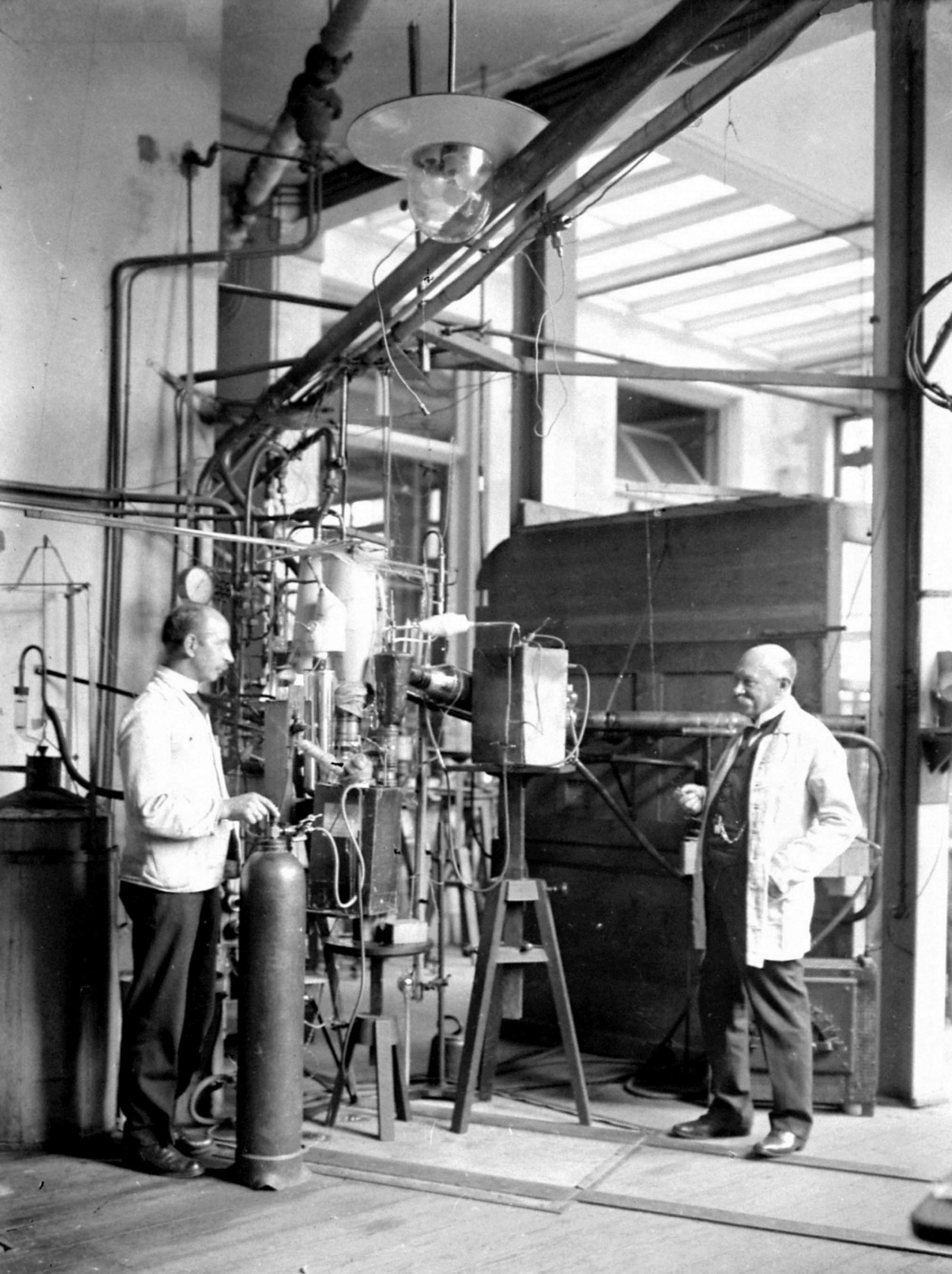

Heike Kamerlingh Onnes
University of Leiden
1908: liquid helium
1911: superconductivity
1913: Nobel prize

$$R_{\mathrm{sc}} < 10^{-16} \times R_{\mathrm{normal}} \; !$$ (1963)

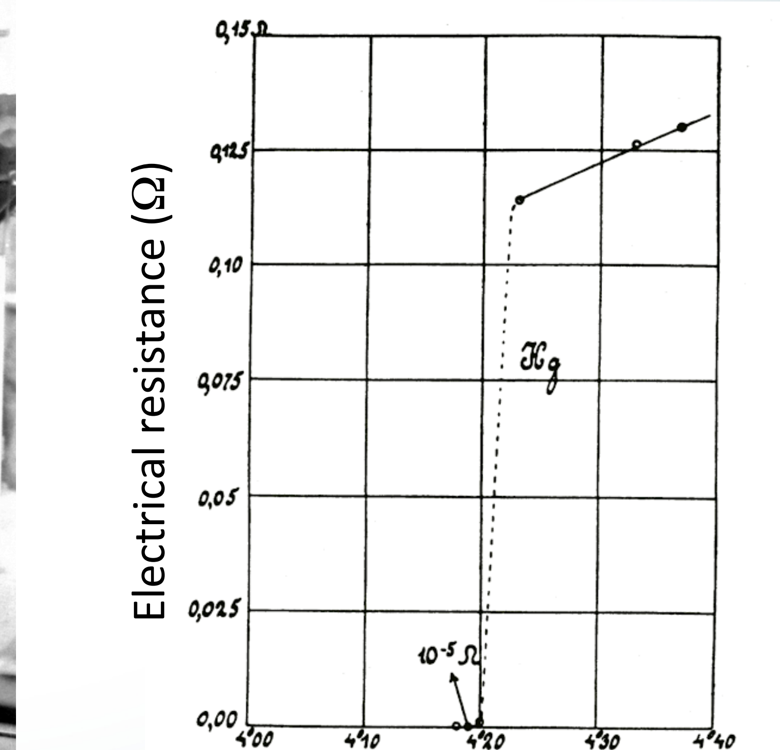

Electrical Conductivity

$$\vec{F} = q\vec{E} - \frac{m}{\tau}\vec{v}$$

scattering time

$$m\vec{a} = m\frac{d\vec{v}}{dt}$$

$$\frac{d\vec{v}}{dt} + \frac{1}{\tau}\vec{v} = \frac{q}{m}\vec{E}$$

Newton's 2^{nd} law

assume:

$$\vec{v}(t) = \mathrm{Re}\left[\vec{v}_0\, e^{j\omega t}\right]$$

$$\vec{E}(t) = \mathrm{Re}\left[\vec{E}_0\, e^{j\omega t}\right]$$

$$\left[j\omega + \frac{1}{\tau}\right]\vec{v}_0\, e^{j\omega t} = \frac{q}{m}\vec{E}_0\, e^{j\omega t}$$

$$\vec{J} = nq\vec{v}$$ Current density

$$\vec{J}_0 = \left[\frac{nq^2\tau}{m}\right]\left[\frac{1}{1+j\omega\tau}\right]\vec{E}_0$$

$$\vec{J} = \sigma\vec{E}$$ Ohm's law – definition of σ

$$\sigma(\omega) = \frac{\sigma(0)}{1+j\omega\tau}$$ Conductivity

$$\sigma(\omega) = \frac{nq^2}{m}\frac{1}{j\omega}$$

Superconductor: $\tau \rightarrow \infty$

Two-fluid model

``superconducting electrons'': $\sigma_{\rm sc}(\omega) = \dfrac{nq^2}{m}\dfrac{1}{j\omega}$

``normal electrons'': $\sigma_{\rm normal}(\omega) = \dfrac{\sigma(0)}{1 + j\omega\tau_{\rm normal}} \approx \sigma(0)$

Superconducting + normal: $\sigma_{\rm total} = \sigma_{\rm sc} + \sigma_{\rm normal}$

$$
\begin{aligned}
Z(\omega) &= \frac{1}{\sigma_{\rm total}(\omega)}\frac{l}{wt} = \frac{1}{\frac{1}{R} + \frac{1}{j\omega L}} \\
&= \frac{j\omega L}{1 + j\omega L/R} \approx j\omega L\,(1 - j\omega L/R) \\
&= +\frac{\omega^2 L^2}{R} + j\omega L
\end{aligned}
$$

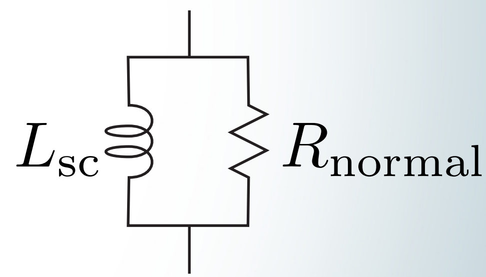

$\text{Note :} \qquad Z(\omega) \to 0 \text{ as } \omega \to 0$

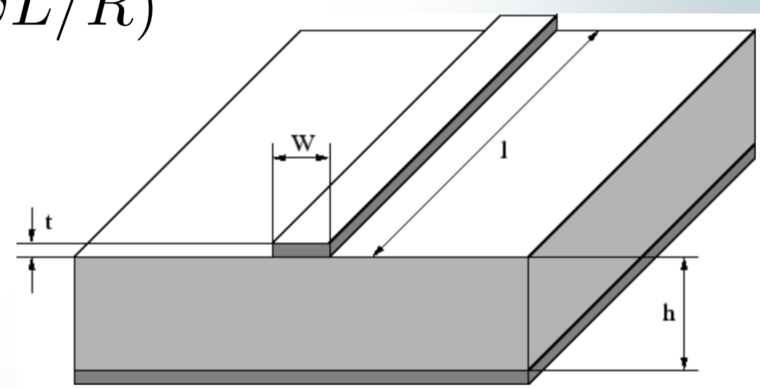

Pair breaking by photons

Pair breaking occurs when:

$$h\nu = \hbar\omega > E_{\mathrm{gap}} = 2\Delta$$

Pair breaking does not occur at microwave frequencies

Pair breaking does occur at far-IR/IR/visible frequencies

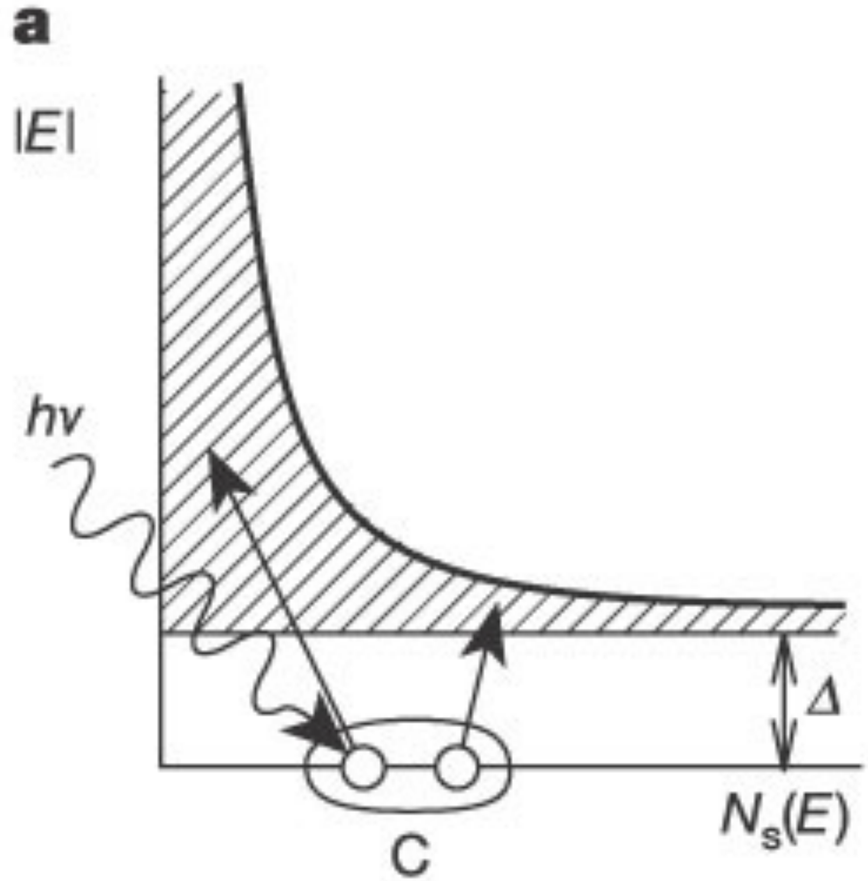

Impedance vs Frequency

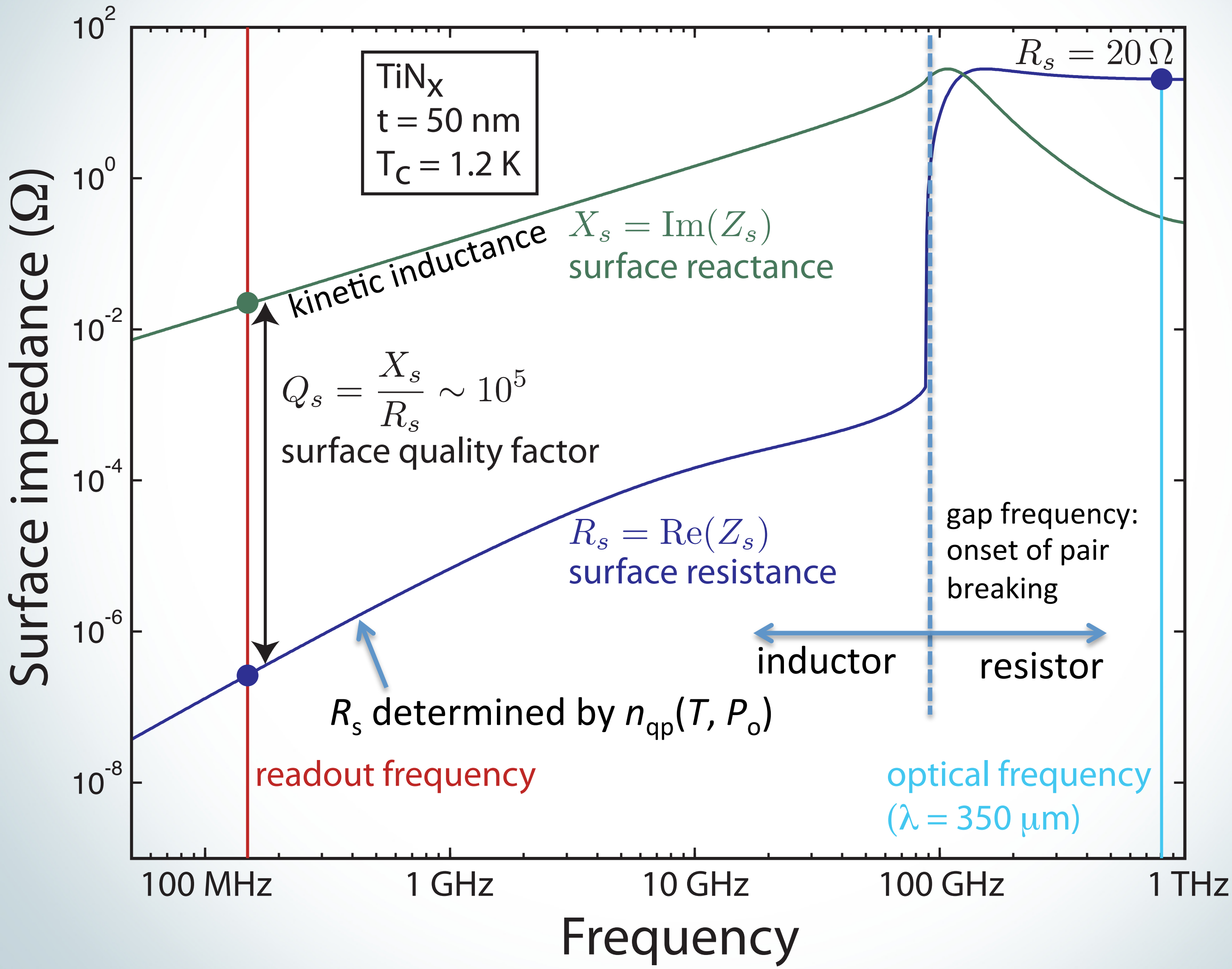

Microwave Kinetic Inductance Detector (MKID)

Cardiff ``LEKID'' pixel
TiN film (gold) on Si substrate (green)

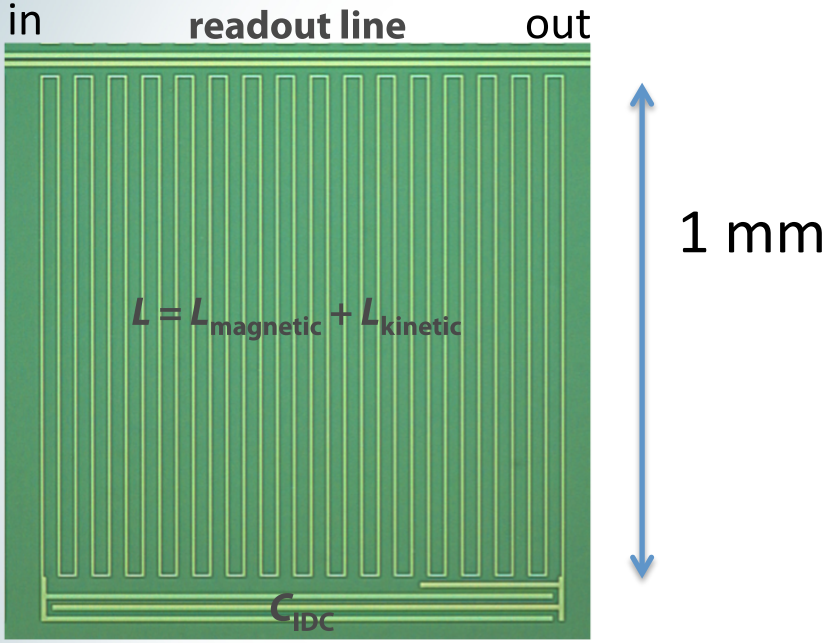

Inductor (L) + capacitor (C) = RF resonator

$$\nu_{\rm r} = \frac{\omega_{\rm r}}{2\pi} = \frac{1}{2\pi\sqrt{LC}} \approx 1\,\mathrm{GHz}$$

TiN inductor is also the optical absorber

- High resistivity: $\rho_{TiN} \sim 500\, \rho_{Al}$ (at 10 K)
- High absorption efficiency
- TiN absorber used in Herschel/PACS bolometers

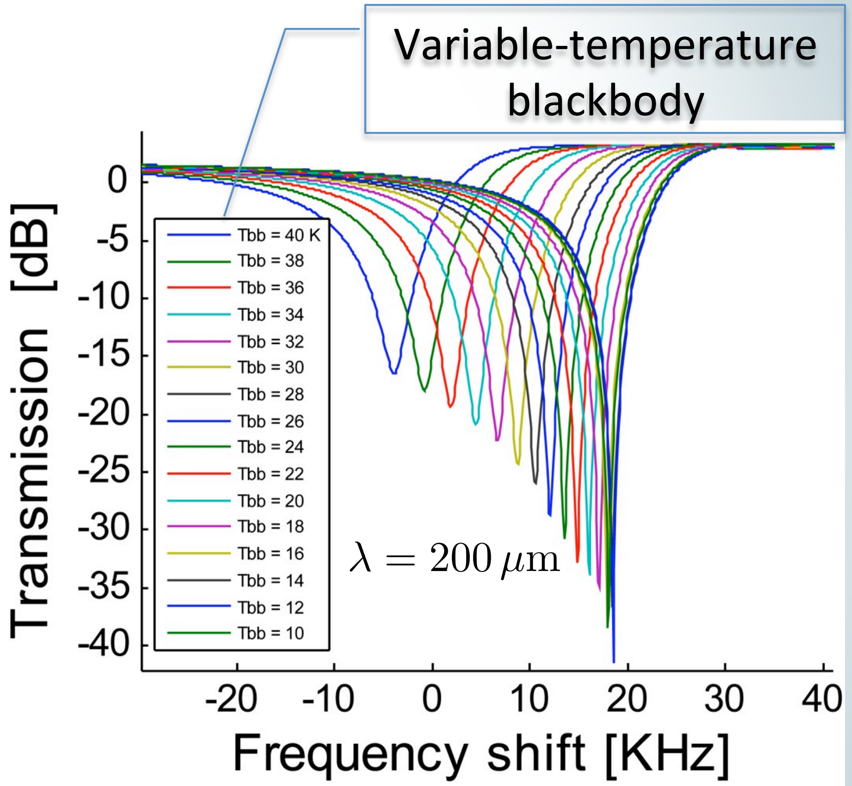

Resonator frequency shifts down as submm radiation is applied

$$\delta x = \frac{\delta\nu_r}{\nu_r} = \frac{1}{2}\frac{\delta L_{\rm kinetic}}{L} \sim \frac{10\,\mathrm{kHz}}{1\,\mathrm{GHz}} = 10^{-5}$$

MKID = Microwave Kinetic Inductance Detector

Frequency multiplexing
(18 x 24 = 432 pixels)

RF In

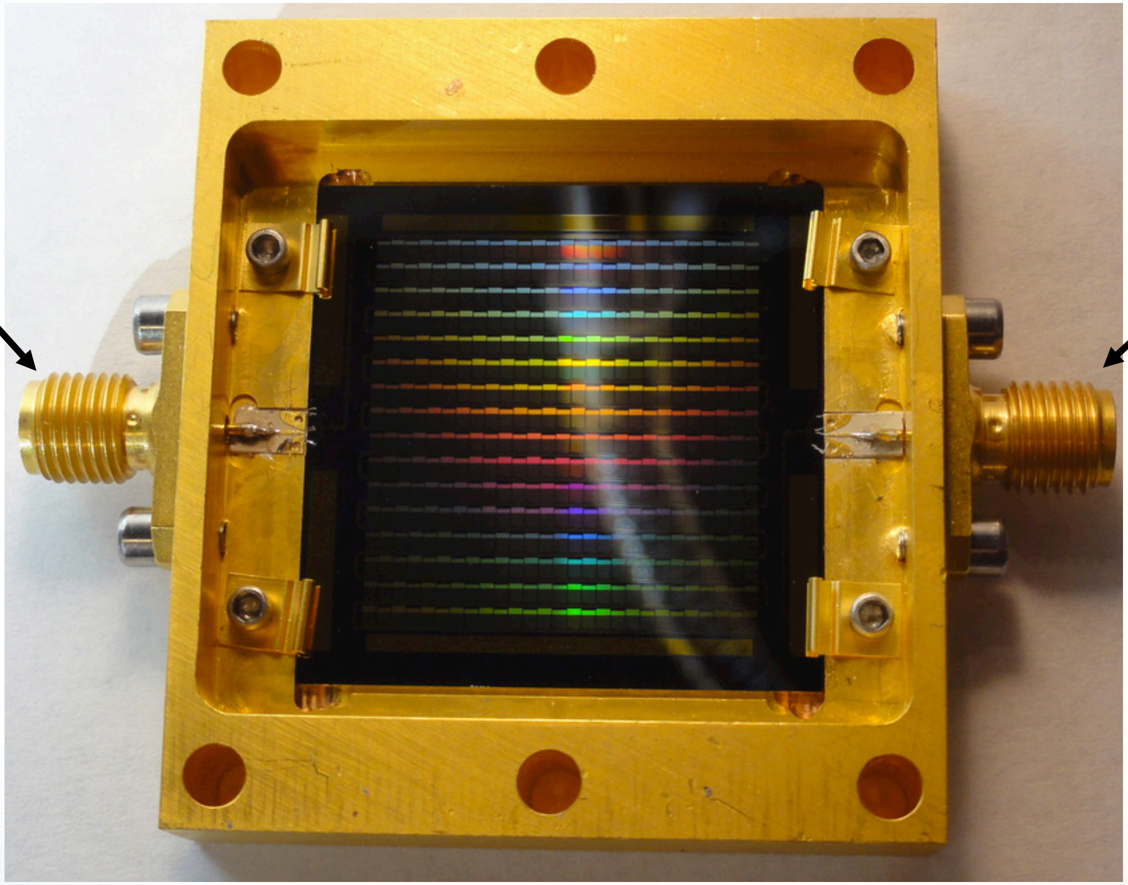

RF Out
(to cryo amp)

Fabrication - Rick Leduc at JPL

Frequency multiplexing
(18 x 24 = 432 pixels)

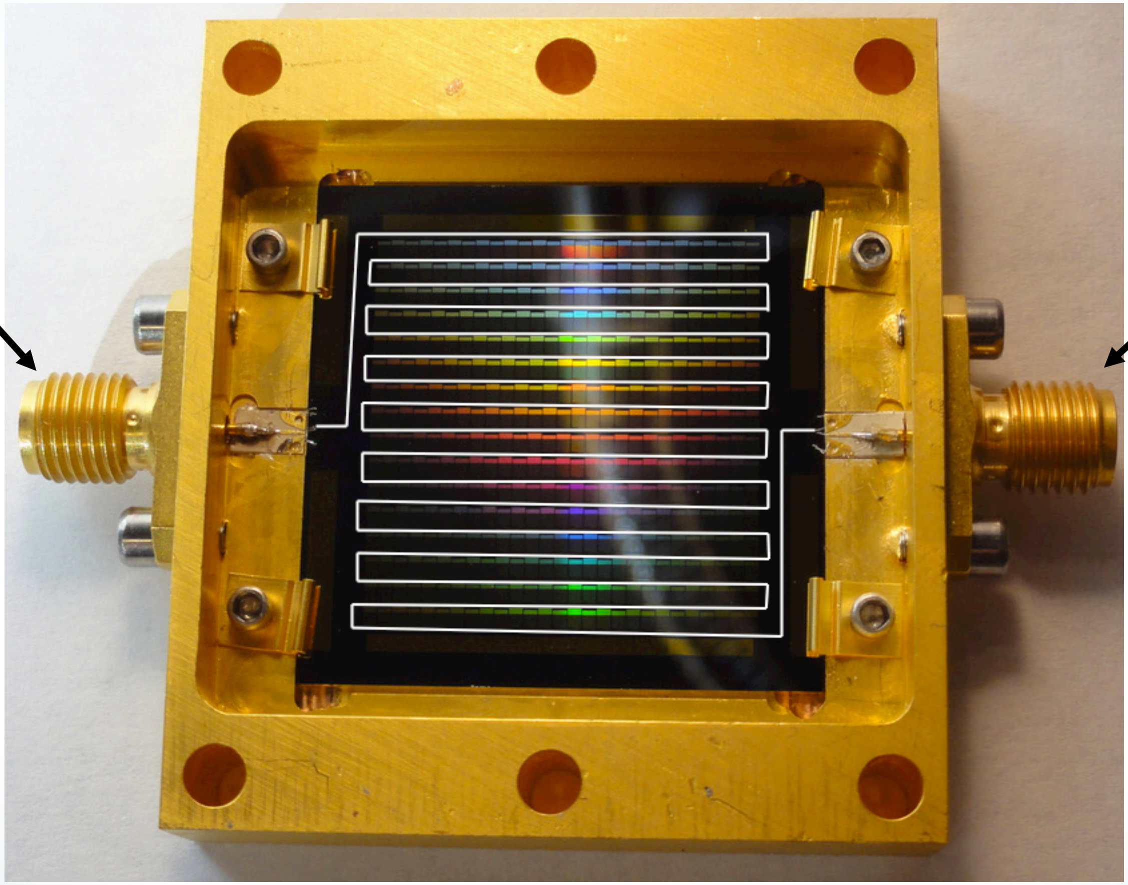

Fabrication - Rick Leduc at JPL

Frequency sweep

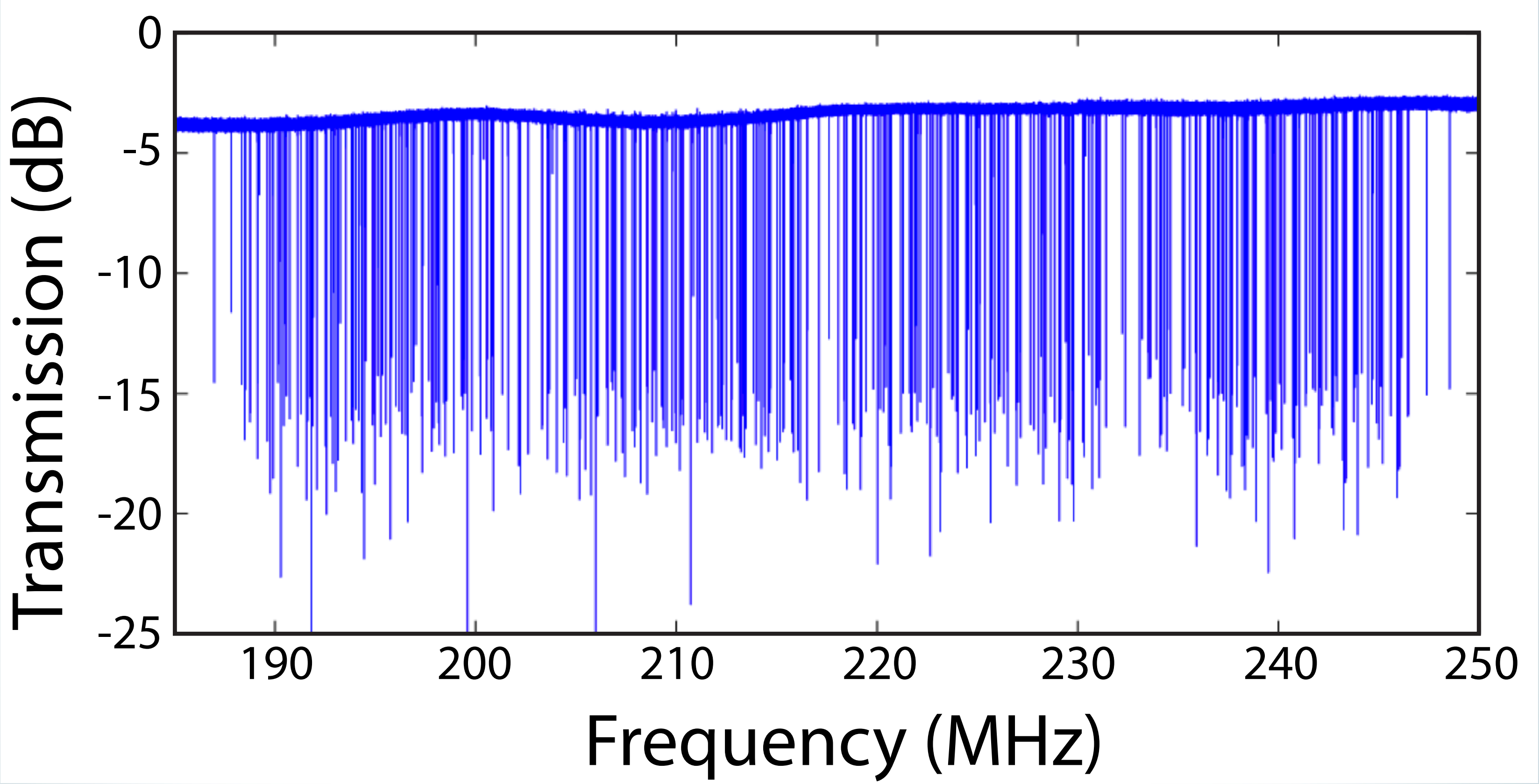

- **Low readout frequency** (200 MHz) enabled by use of TiN (large ρ_n → large L_k)
- Resonator frequencies span 185-250 MHz (65 MHz bandwidth or 0.43 octaves)
- 415/432 resonators deeper than 6 dB (96% yield)
- 160 kHz average spacing

Resonator Q sets mux density

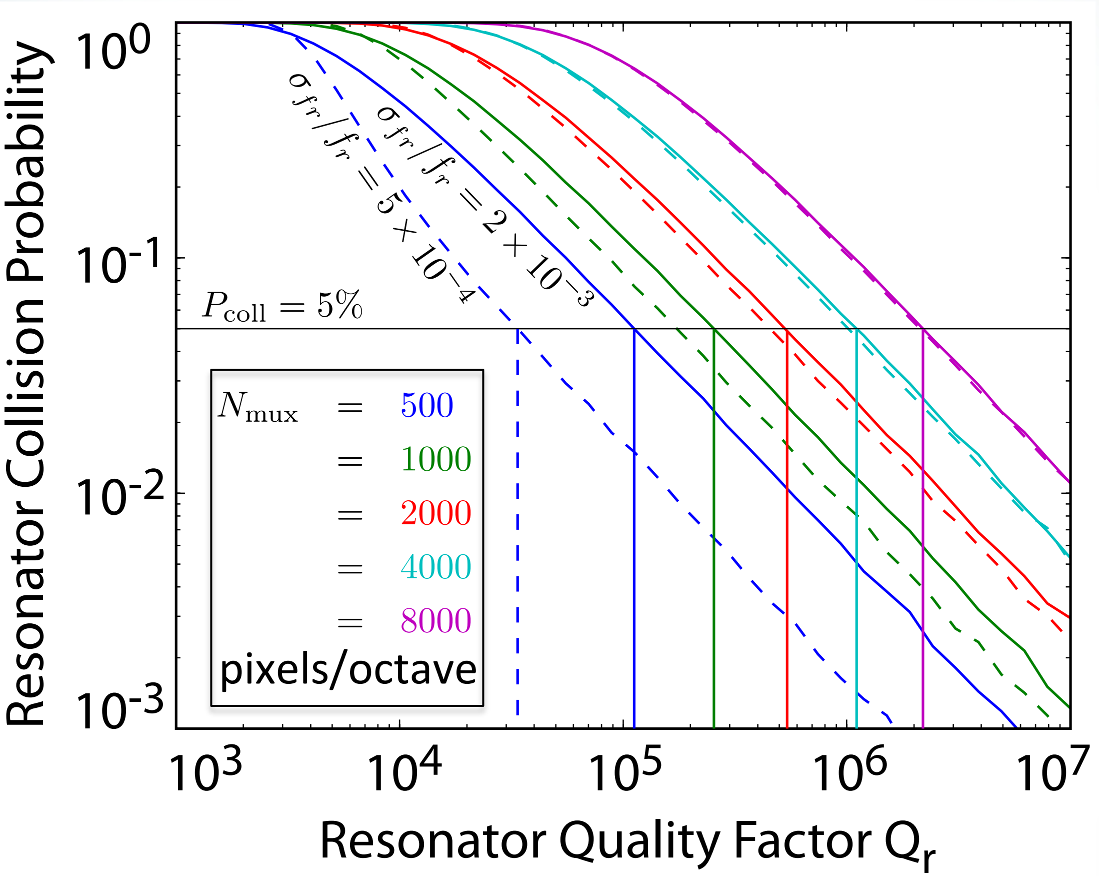

$$\frac{1}{Q_r} = \frac{1}{Q_c} + \frac{1}{Q_i}$$

- High Q_r → low collision probability
  - Do not rely on precise placement of resonator frequencies (σ_f)
  - Collision probability independent of σ_f for high mux density
- Need $Q_r \sim 10^5$ to multiplex 500-1000 pixels/octave
- Previous slide: 432 pixels / 0.43 octave = 994 pixels/octave @ 96% yield

Multichannel Digital Readout

CCAT

- FPGA implements digital channelizer for readout tone separation
- Microwave (GHz) readout requires up/down frequency conversion
- RF readout (< 500 MHz) allows ``direct drive'' with ADC/DAC
  - Reduces readout bandwidth, complexity, and cost
  - Converters are typically 12-bit, 500 MSPS (ADC < $200 ea)
  - **Use frequency readout** since $\beta = \delta x / \delta Q^{-1} \sim 50 \quad (\propto 1/\omega_r)$

Microwave readout

RF readout

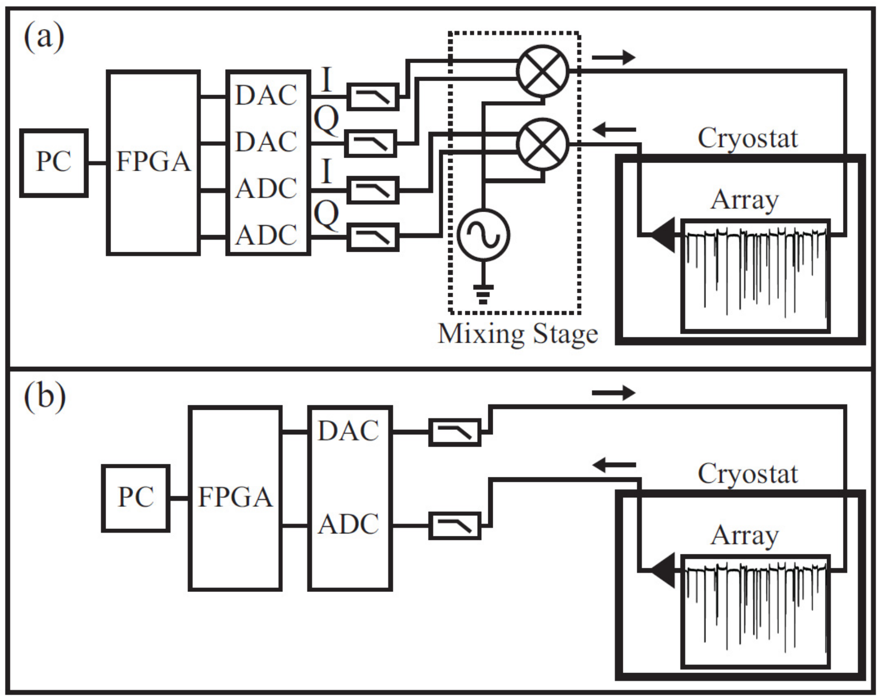

L. Swenson, LTD-15 2013

CIT/JPL Development Timeline

- 1987: kinetic inductance bolometer proposed (McDonald/NIST)
  - SQUID readout
- 1999: ``modern'' KIDs proposed (Zmuidzinas & Leduc)
  - Microresonator as pair-breaking detector, $T \ll T_c$ operation, vector RF/microwave readout, cryogenic transistor LNA, frequency multiplexing
- 2003: lab demo of x-ray detection (Day *et al*., Nature)
  - Excess noise measured, origin not understood
- 2008: excess noise produced by resonator capacitor
  - due to surface layer of TLS fluctuators (Gao *et al*., APL)
- 2010: TiN introduced, high *Q* demonstrated (Leduc *et al*., APL)
  - High resistivity → THz LEKID absorber, high KI fraction, 100-200 MHz readout
- 2012: interpixel EM coupling and its cure (Noroozian *et al.*, IEEE MTT)
- 2013: operation into deep nonlinear KI regime (Swenson *et al*. JAP)
- 2013: 432-pixel, 350 μm MAKO camera demonstrated on CSO (April)
  - CCAT PDR (September)
- 2014: NbTiN resonator bolometer demonstrated (Swenson *et al*., in prep.)

Sensitivity

- Determined by responsivity R_x and noise S_x
  - Noise equivalent power (NEP)

$$\mathrm{NEP}(\nu) = \frac{\sqrt{S_x(\nu)}}{\mathcal{R}_x(\nu)} \qquad \mathrm{W\,Hz^{-1/2}}$$

  - Fractional frequency responsivity

$$\mathcal{R}_x = \frac{dx}{dP_\mathrm{o}} \qquad \mathrm{W^{-1}}$$

(rolls off due to τ_{qp}, τ_r)

  - Fractional frequency noise power spectral density

$$S_x(\nu) = \mathrm{PSD}_x(\nu) = \left\langle \left|\mathrm{FFT}\left[\delta x(t)\right]\right|^2 \right\rangle \qquad \mathrm{Hz^{-1}}$$

(σ_x^2 in 1 Hz BW around ν)

- Detector NEP should be below photon NEP
  - Increase responsivity and/or reduce noise

Responsivity model

CCAT

- Optical power produces quasiparticles:

$$\delta N_{\rm qp} = \frac{\eta_o \delta P_o}{\Delta} \tau_{\rm qp}$$

τ_{qp} depends on material, T_c, optical load…

- Quasiparticles cause frequency shift:

$$\delta x = \frac{\delta f_r}{f_r} = \frac{1}{2}\frac{\delta L_{\rm kinetic}}{L} = \frac{1}{2}\frac{L_{\rm kinetic}}{L}\frac{\delta L_{\rm kinetic}}{L_{\rm kinetic}} \sim \frac{1}{2}\alpha\frac{\delta N_{\rm qp}}{2N_0\Delta V_L}$$

kinetic inductance fraction

single-spin electron density of states

- Responsivity is given by:

$$\mathcal{R}_x = \frac{dx}{dP_o} = \frac{\alpha\gamma S_2 \eta_o \tau_{\rm qp}}{4N_0\Delta^2 V_L}$$

$$\alpha\gamma S_2 \eta_o \sim 0.5 - 1$$

Optical to qp energy conversion efficiency

- **Rely on measurements** of R_x
  - Adjust N_0 to match measurements
- Methods to boost responsivity:
  - reduce T_c (smaller Δ, larger τ_{qp})
  - reduce inductor volume V_L (smaller absorber → microlenses)
  - (recycle phonon energy - place inductor on thermal island)
    - effectively increases τ_{qp}

Noise model

- Random fluctuations of quasiparticle population
  - Photon arrivals
    $$\mathrm{NEP}^2_{\mathrm{photon}} = 2P_o h\nu(1+n_o)$$
  - qp recombination
    $$\mathrm{NEP}^2_{\mathrm{g-r}} = \frac{4\Gamma_{\mathrm{th}}\Delta^2}{\eta_o^2} + \frac{2N_{\mathrm{qp}}\Delta^2}{\eta_o^2}(\tau_{\mathrm{max}}^{-1}+\tau_{\mathrm{qp}}^{-1})$$
- Readout noise
  - Dominated by first-stage cryo amplifier
    $$S_x^{\mathrm{amp}} = \frac{kT_{\mathrm{amp}}}{P_g}\frac{Q_c^2}{4Q_r^4}\ .$$
  - For simplicity, keep generator power P_g below bifurcation

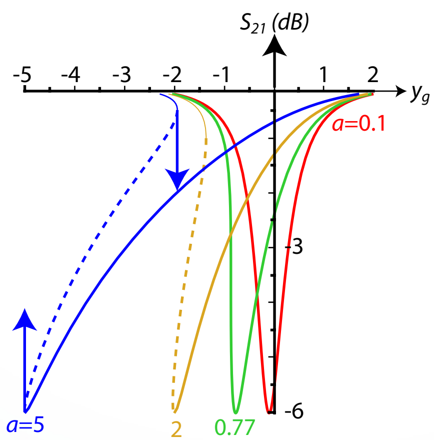

Swenson et al 2013

- Capacitor noise
  $$S_x = \mathrm{PSD}(\delta C/2C)$$

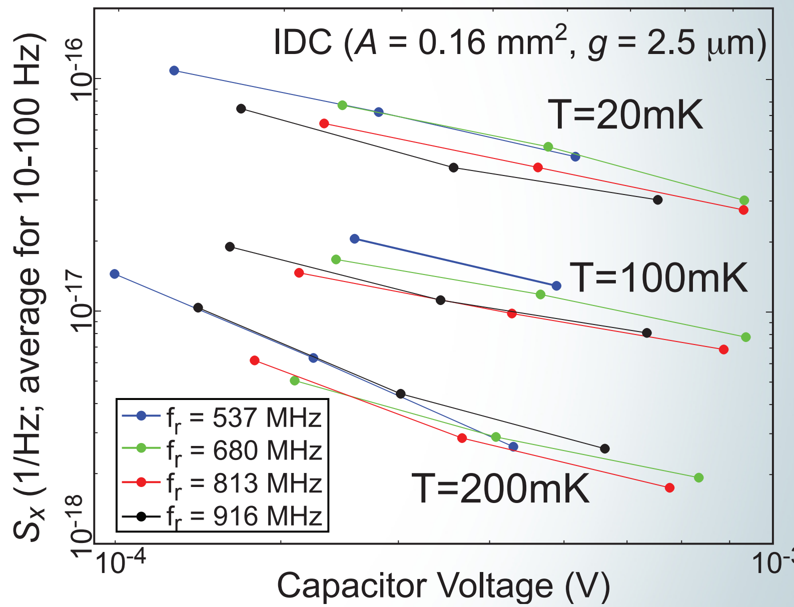

Array Design Details

Ver	Layout	Opt. Couple	Inductor				Capacitor		Freq	Lith Steps	Pixels	Pol.
			Area	Trace	Sep	t	Area	Sep				
			mm^2	μm	μm	nm	mm^2	μm	MHz			
1G	Square	Bare	0.64	4	8	50	<0.4	2	170-240	3	432	1
2G	Hex $1mm^2$	μLens (F/2)	0.3	2	4	50	0.6	2-6	200-240	2	488	1
3G	Hex $1mm^2$	μLens (F/2)	0.3	1	9	100	0.6	4-9	100-150	2	488	2

- 1G: Tested at CSO (MAKO)
- 2G: Currently lab testing
- 3G: Design phase

350 μm Pixel Design (TiN 1G)

- CSO/MAKO demonstration
- LEKID pixel style (Doyle et al 2007)
  - F# and λ set absorber size:
    - Fλ / 2 ~ 0.8 mm
  - Matching of absorber to wave impedance in silicon (90 Ω) determines TiN fill factor and volume of inductor/absorber
  - Capacitor area: trade-off between readout frequency & capacitor noise vs focal plane filling efficiency
  - 432 pixels fills one stepper field
    - Allows rapid iteration

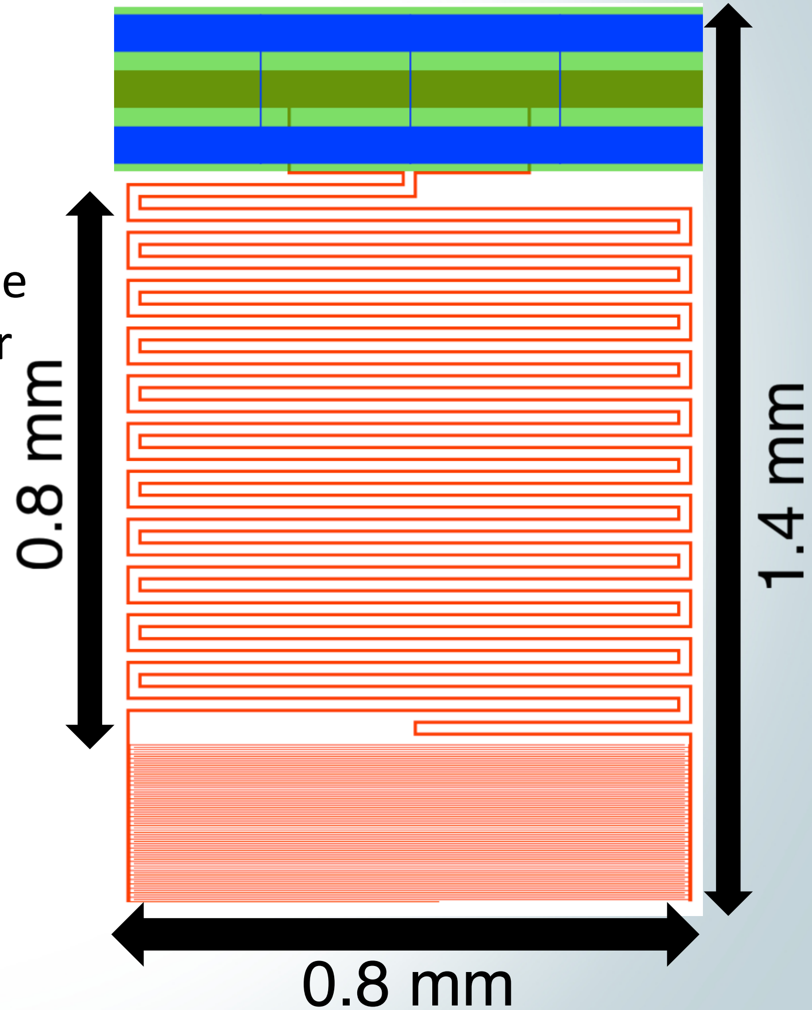

TiN 1G: 432-pixel array

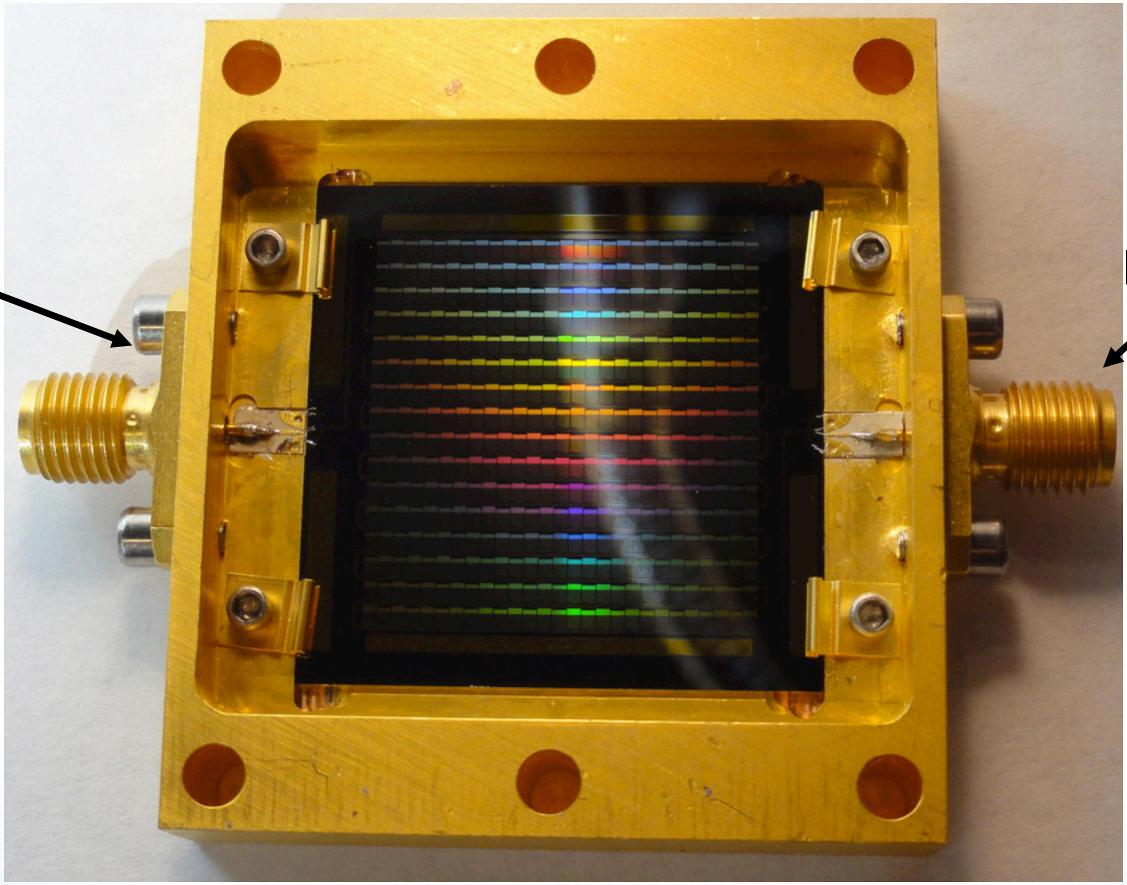

Fabrication - Rick Leduc at JPL

TiN 1G - frequency sweep

- Measurements results were promising:
  - MUX density: ~ 500 pixels/half octave
  - High yield (> 95% visible, >90% with usable spacing)
  - Uniform coupling and low ripple on transmission line

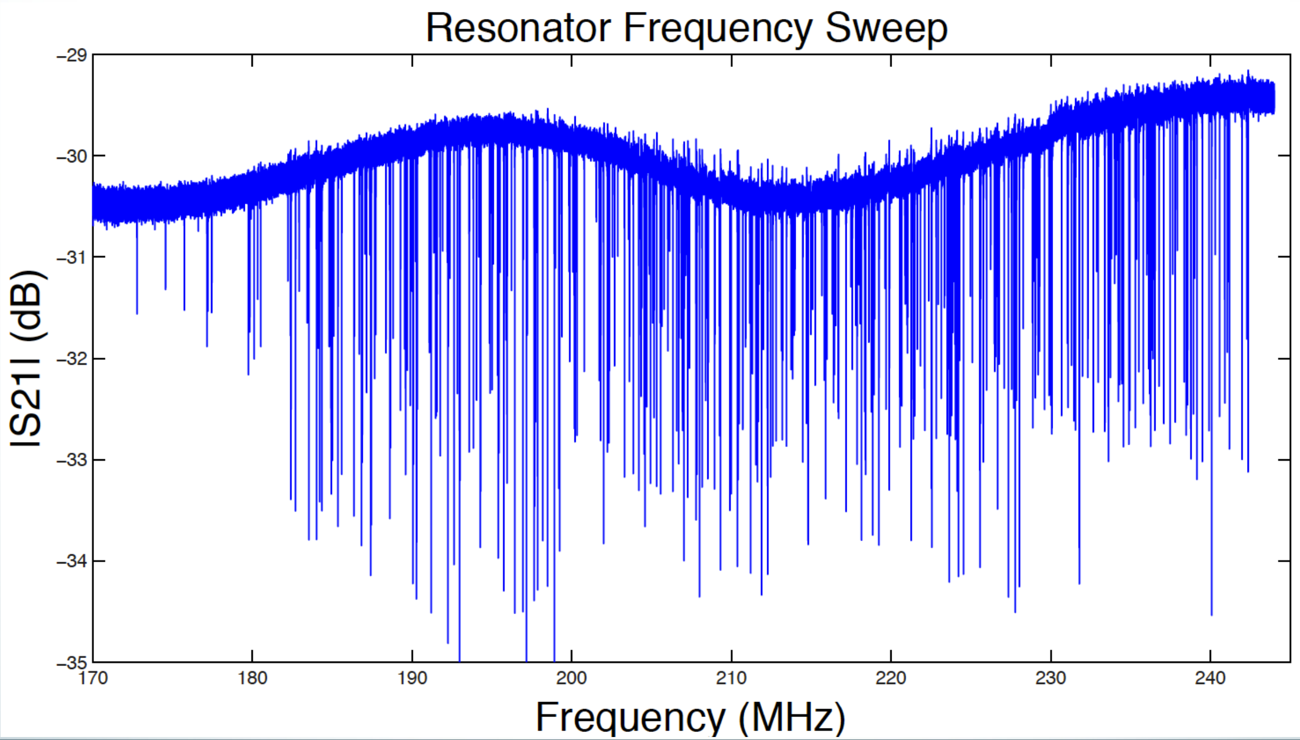

TiN 1G – Coupling Q

- Very uniform coupling Q
  - Design value: 2×10^5

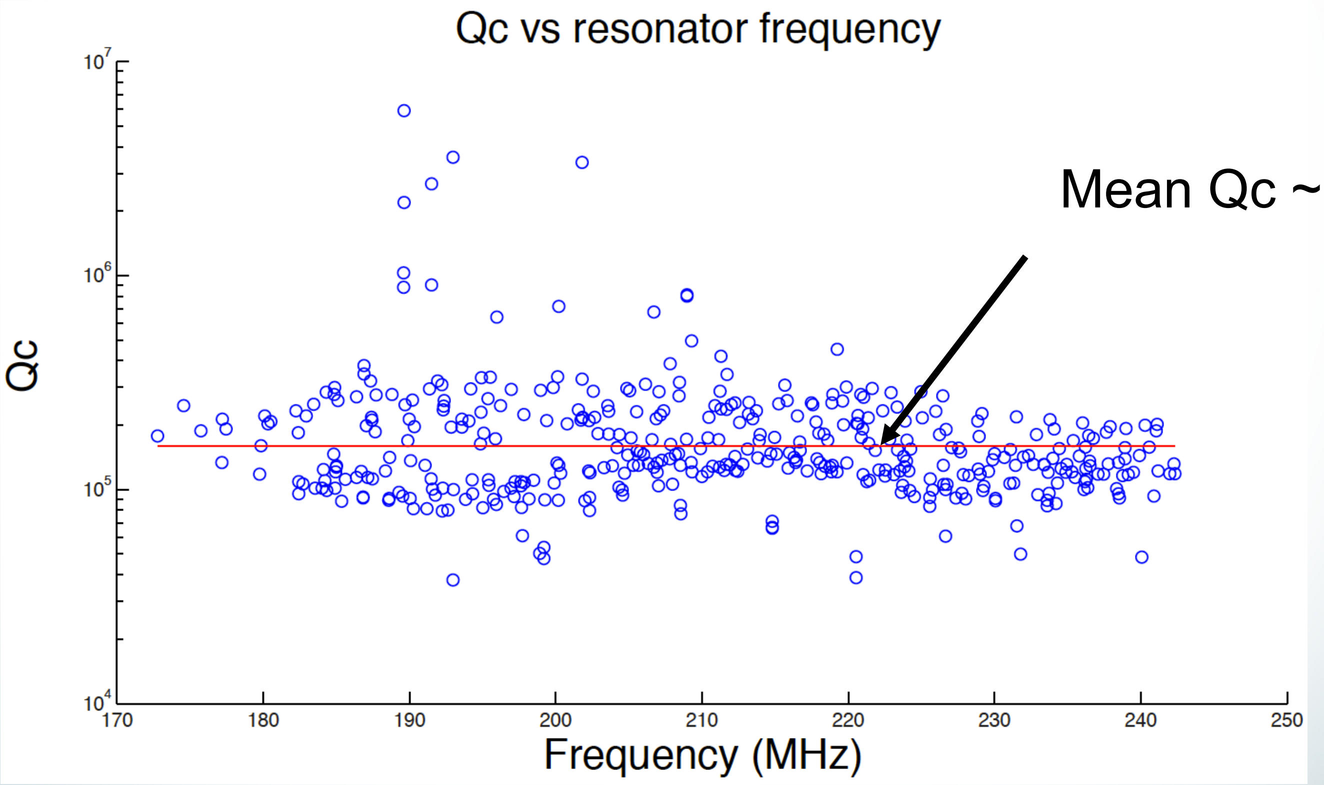

TiN 1G: Lab Noise Measurement

- Mounted in dilution refrigerator
  - Cold blackbody, filters at 212 μm

$$\frac{h\nu}{k_B} = 68\,\mathrm{K}$$

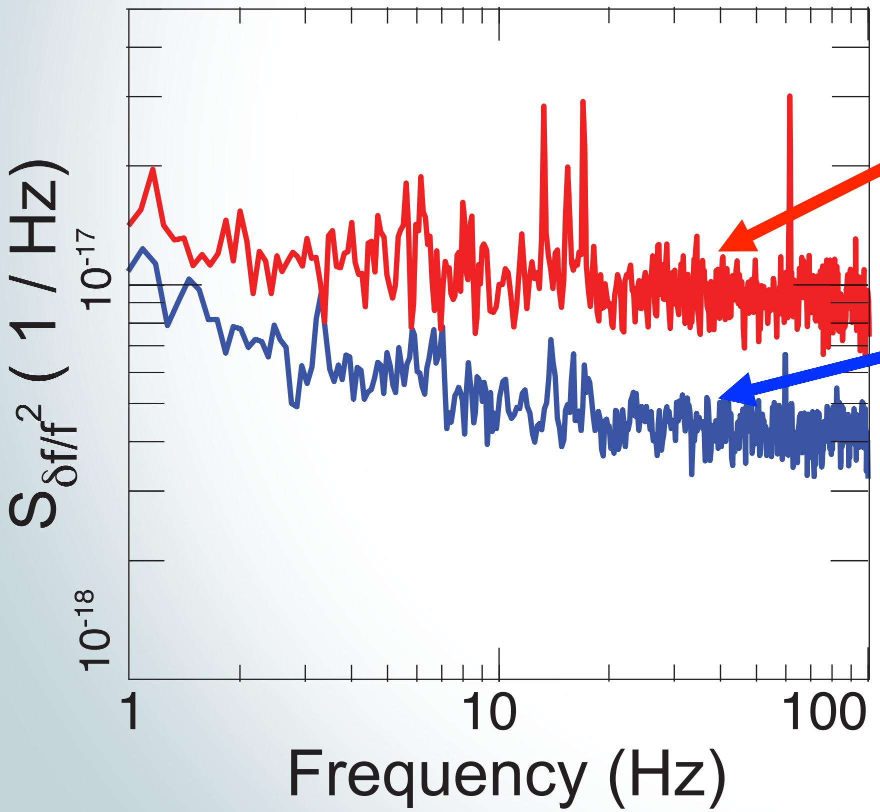

T_{BB} = 35 K, Pinc ~ 120 pW

T_{BB} = 25 K, Pinc ~ 50 pW

- Photon noise visible to a few Hz
- Optical efficiency ~ 0.7
- Capacitor noise dominates below 1 Hz
- Loading higher than CSO
- Predict ~ 2-3x photon NEP at CSO (for single polarization)

MAKO: a prototype camera

(Swenson et al, SPIE Proc., 2012)

CCAT

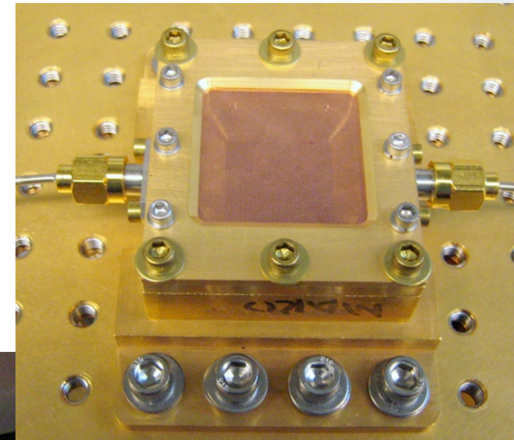

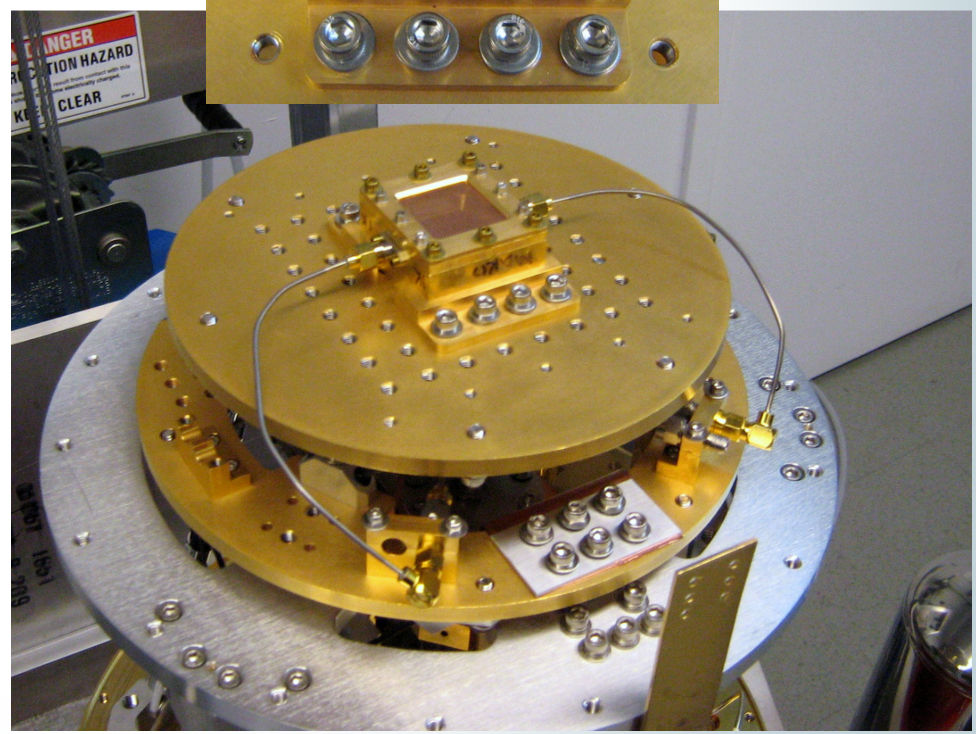

MAKO In Lab

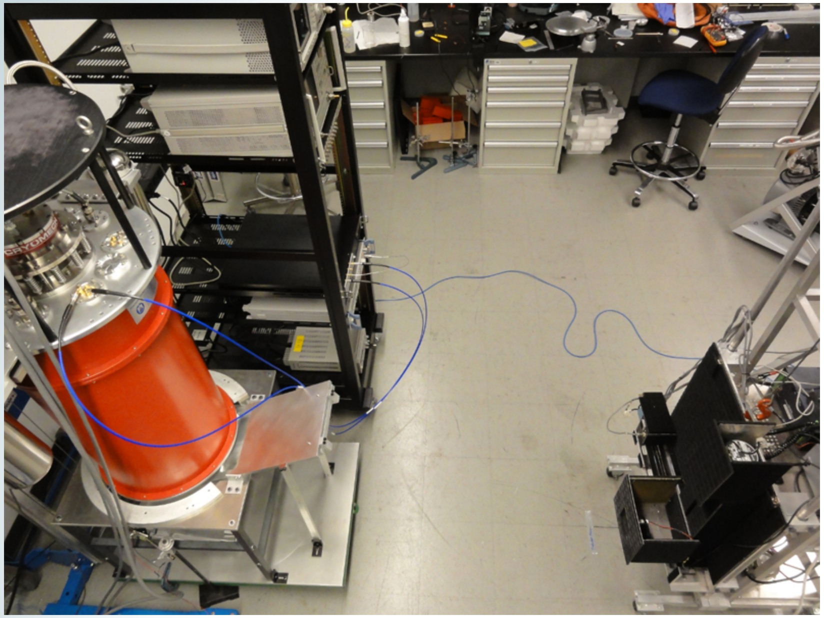

MAKO In lab:

- Mounted on optics to mimic SHARC-II
- ROACH board + clock on electronics rack
- Beam mapper placed at focus to test point source response

Cryostat cold head

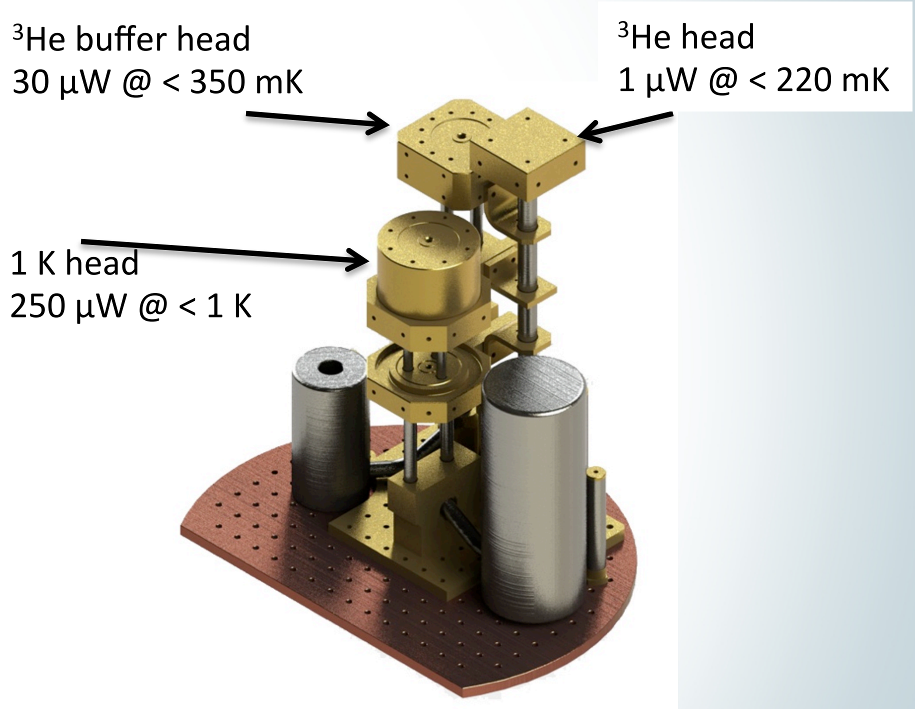

- Cryostat by Precision Cryogenics
- PT410 Pulse tube cooler
- 3He system
  - base T 240mK under loading
  - hold time ~ 36 hours

MAKO Optics

	Absorber Size	# Pixels	Polarizations	Backshort?
	(mm^2)	(nominal)		
SHARC-II	1 x 1	384	2	yes
Mako	0.8 x 0.8	432	1	no

- *A SHARC-II pixel receives 4.4x more optical power compared to a MAKO pixel*

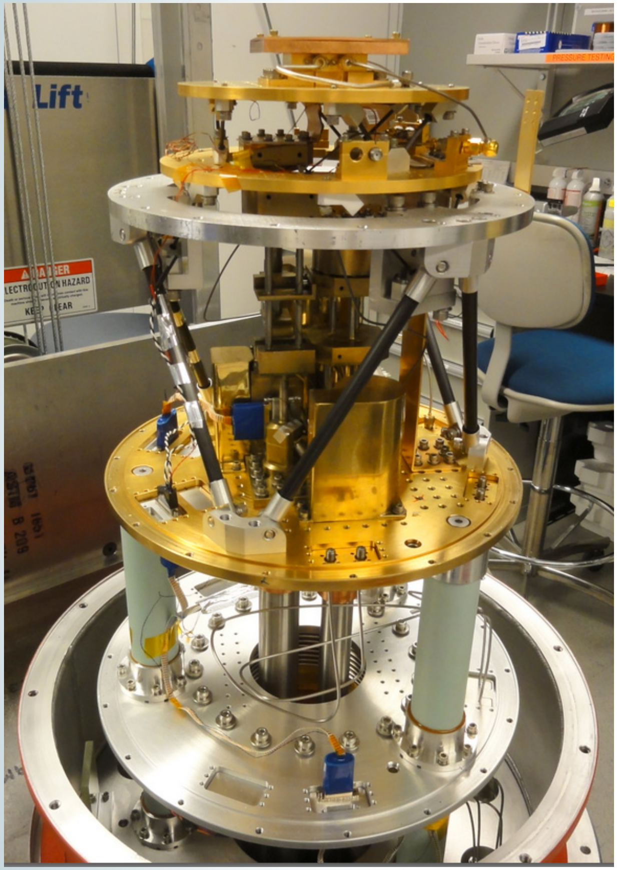

MAKO cryostat: optics designed to closely match CSO's SHARC-II camera

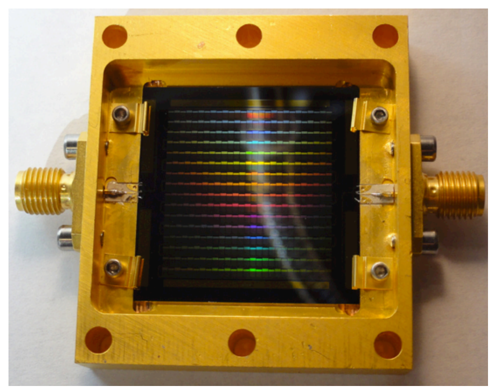

MAKO detector array (multiplexed)

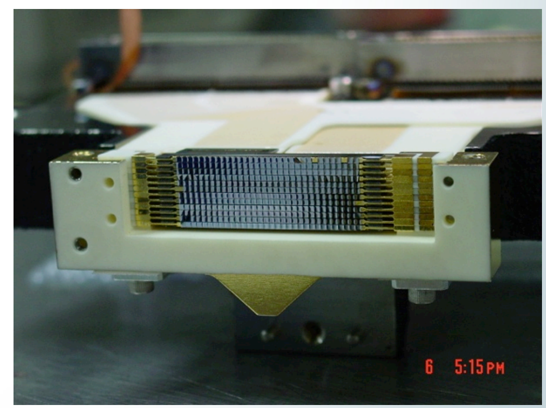

SHARC-II detector array (individually wired)

MAKO goes to the CSO

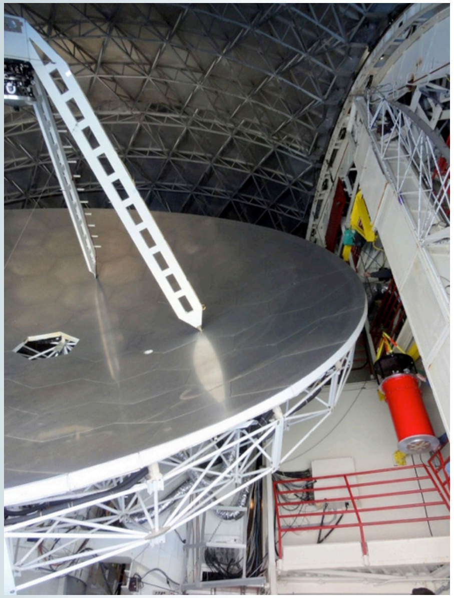

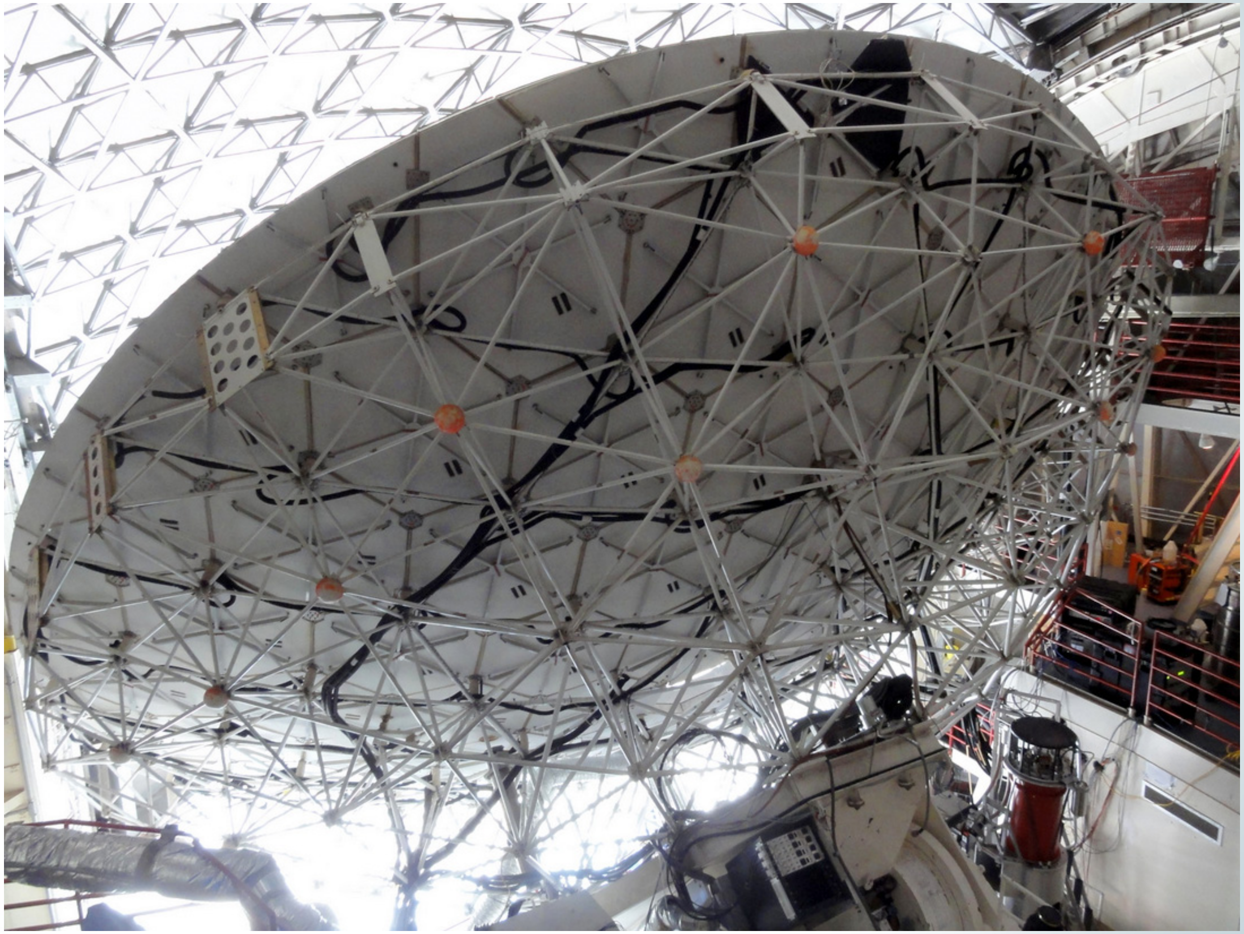

MAKO goes to the CSO

CCAT

10 MHz rubidium standard & 1 PPS Signal
(from GPS antenna)

Amp
Bias

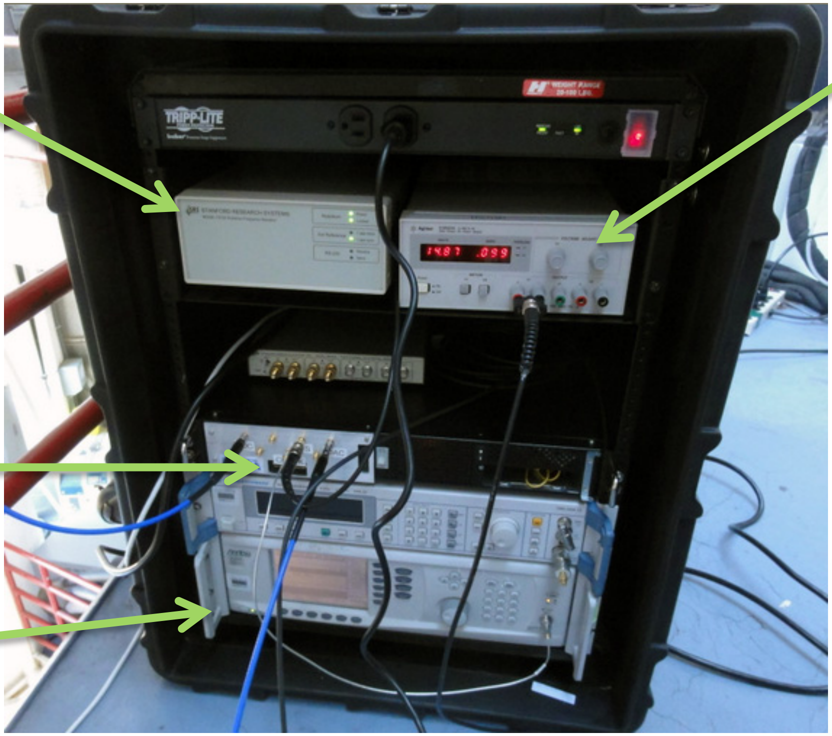

ROACH

Roach Clock
(500 MSPS)

10 MHz standard, Clock, and Amp bias can be shared by multiple ROACH readouts

MAKO Readout Electronics

- ROACH Readout
  - Open-source FPGA readout (CASPER/Berkeley)
  - Adopted existing hardware to meet observing date
  - Maximum readout frequency: 250 MHz
    - 500 MSPS ADC converters operating in 1st Nyquist zone

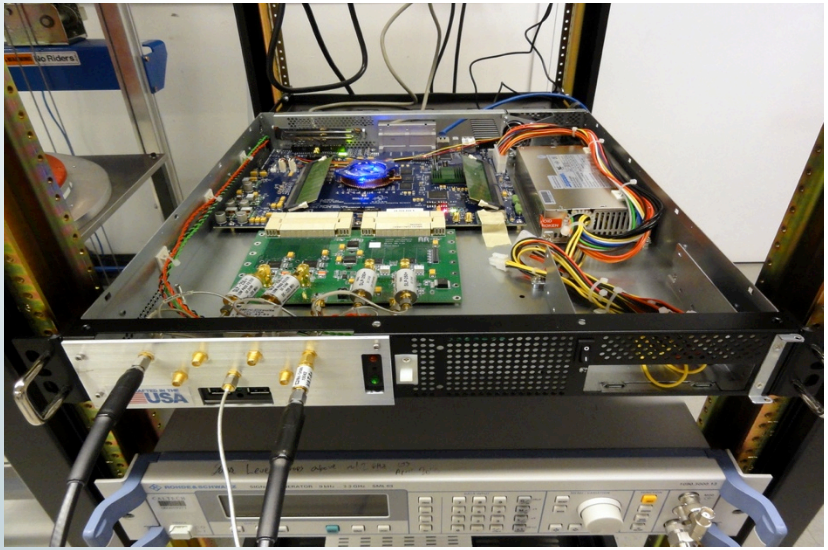

- MAKO implemented with ~ 500 pixels with one ADC and one DAC
- FPGA firmware supports up to 4k pixels per ROACH
- FPGA firmware developed by R. Monroe/JPL

MAKO goes to the CSO

- Front end software:
  - Calibration and measurement of IQ streams
  - Found > 95% of designed pixels

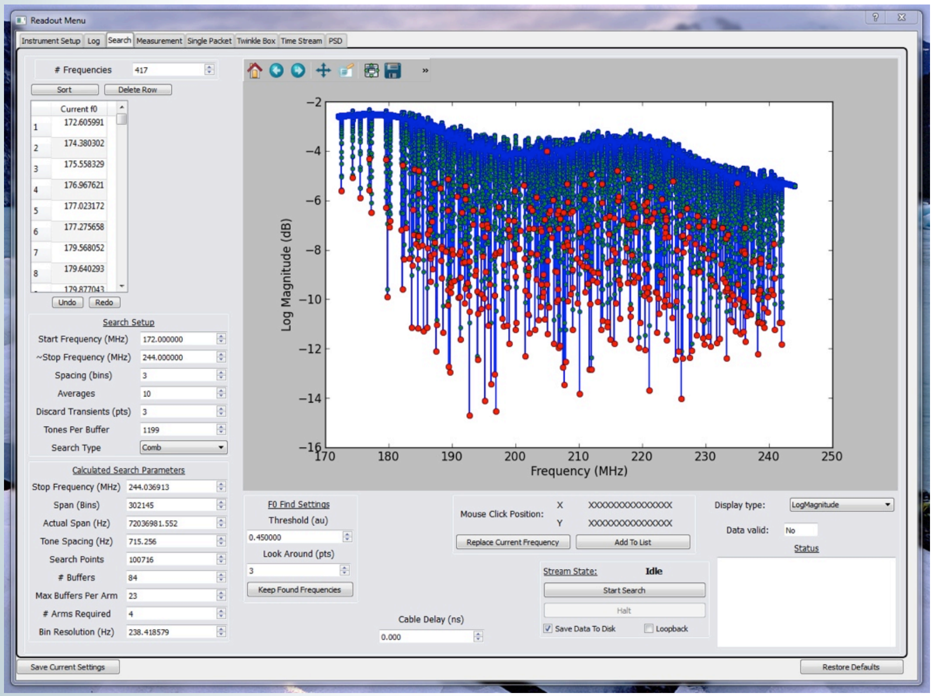

Readout interface and visualization software developed by L. Swenson

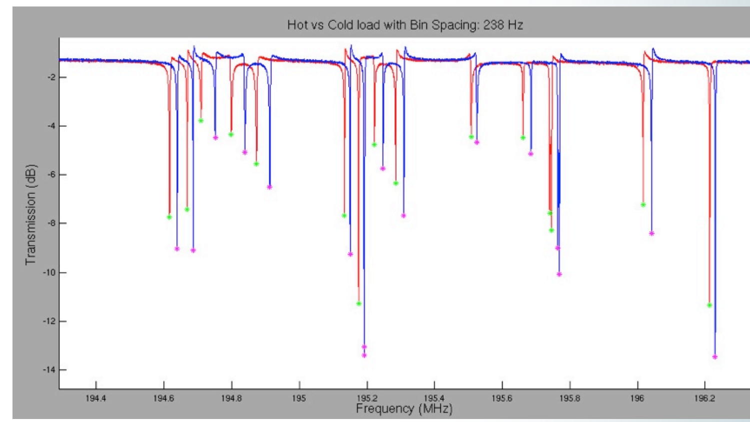

300 K vs **77 K** load

MAKO goes to the CSO

- First Light on the first night of observing!

Photo by L. Swenson

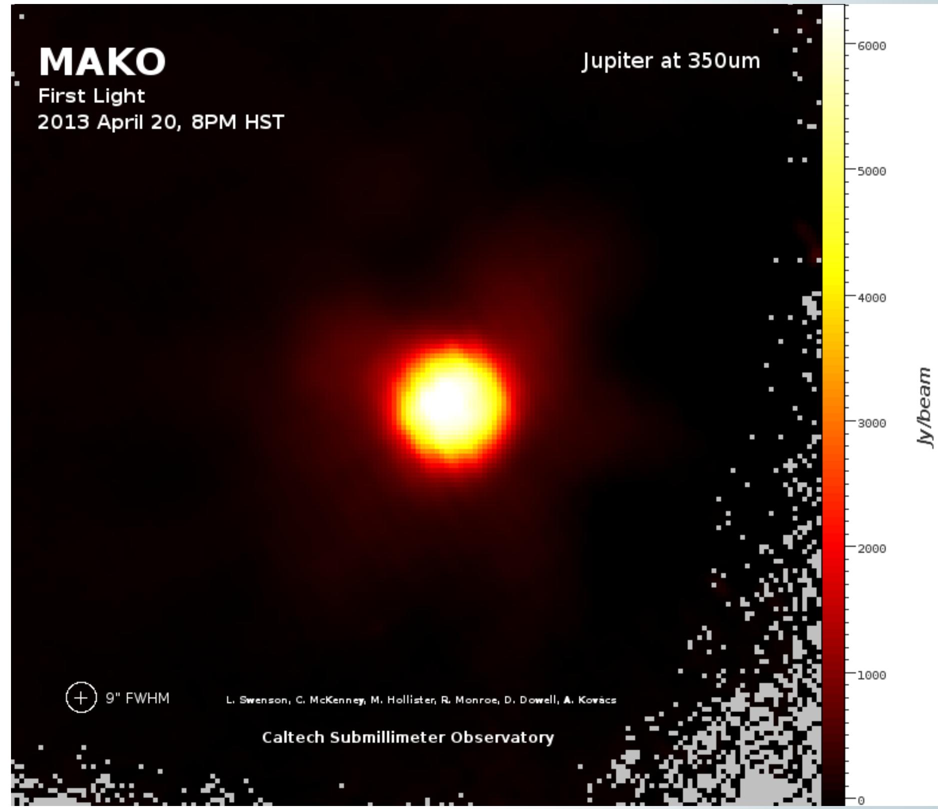

MAKO goes to the CSO

- Some decent weather nights:

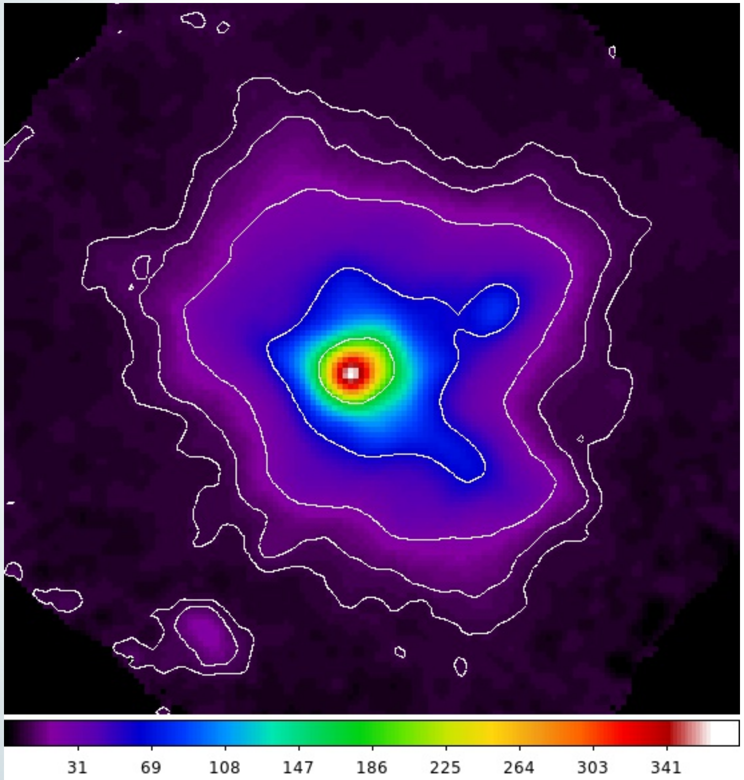

G34.3

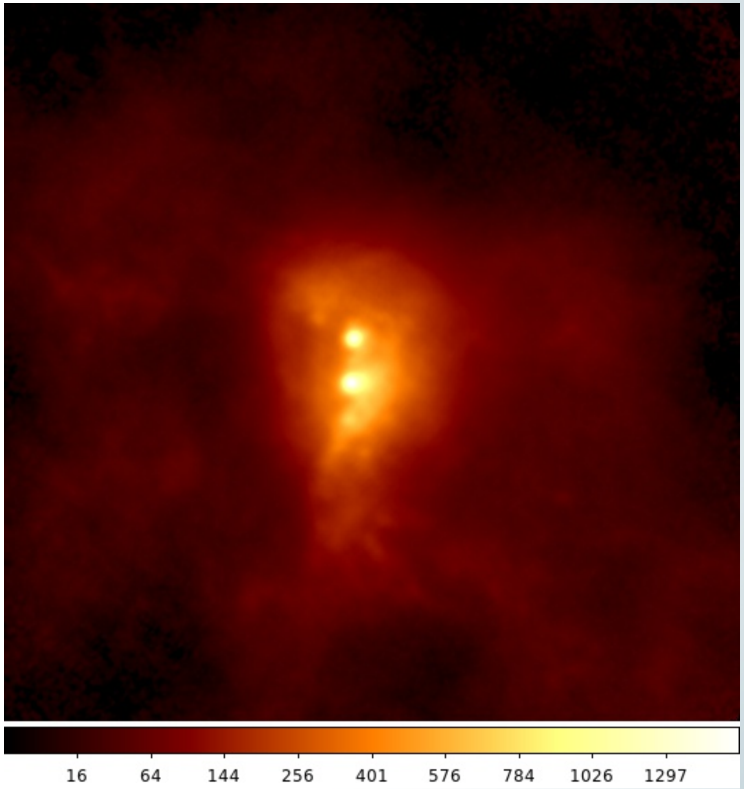

SgB2

MAKO goes to the CSO

- And on poor weather nights…

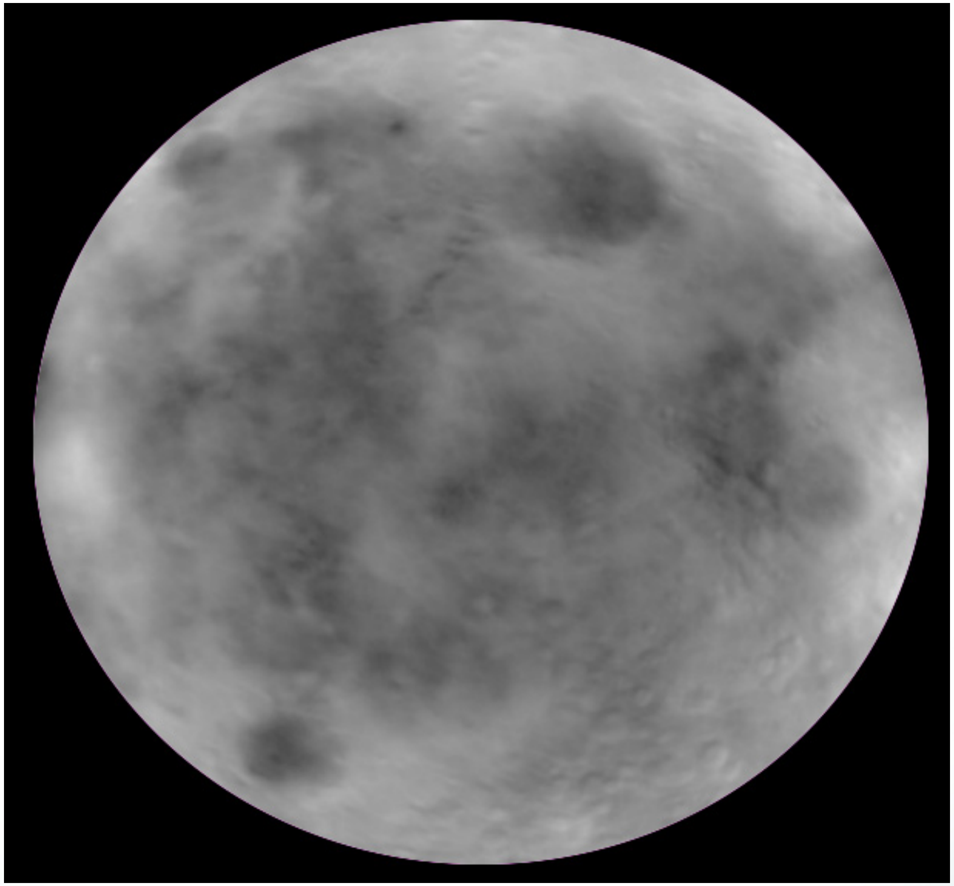

The moon at λ = 350 μm

Back in the Lab

- MAKO NEFD was ~ 8x that of SHARC-II
  - Was expected to be detector noise limited
  - Recall Sharc-II pixels receive 4.4x more light
- Second-generation arrays (TiN 2G)
  - Lower NEP & NEFD: reach BLIP
  - Increased responsivity (smaller volume → microlenses)
  - Reduced capacitor noise (larger area, increased electrode separation)
  - Better uniformity (Tc)

Second-generation 484-pixel TiN array

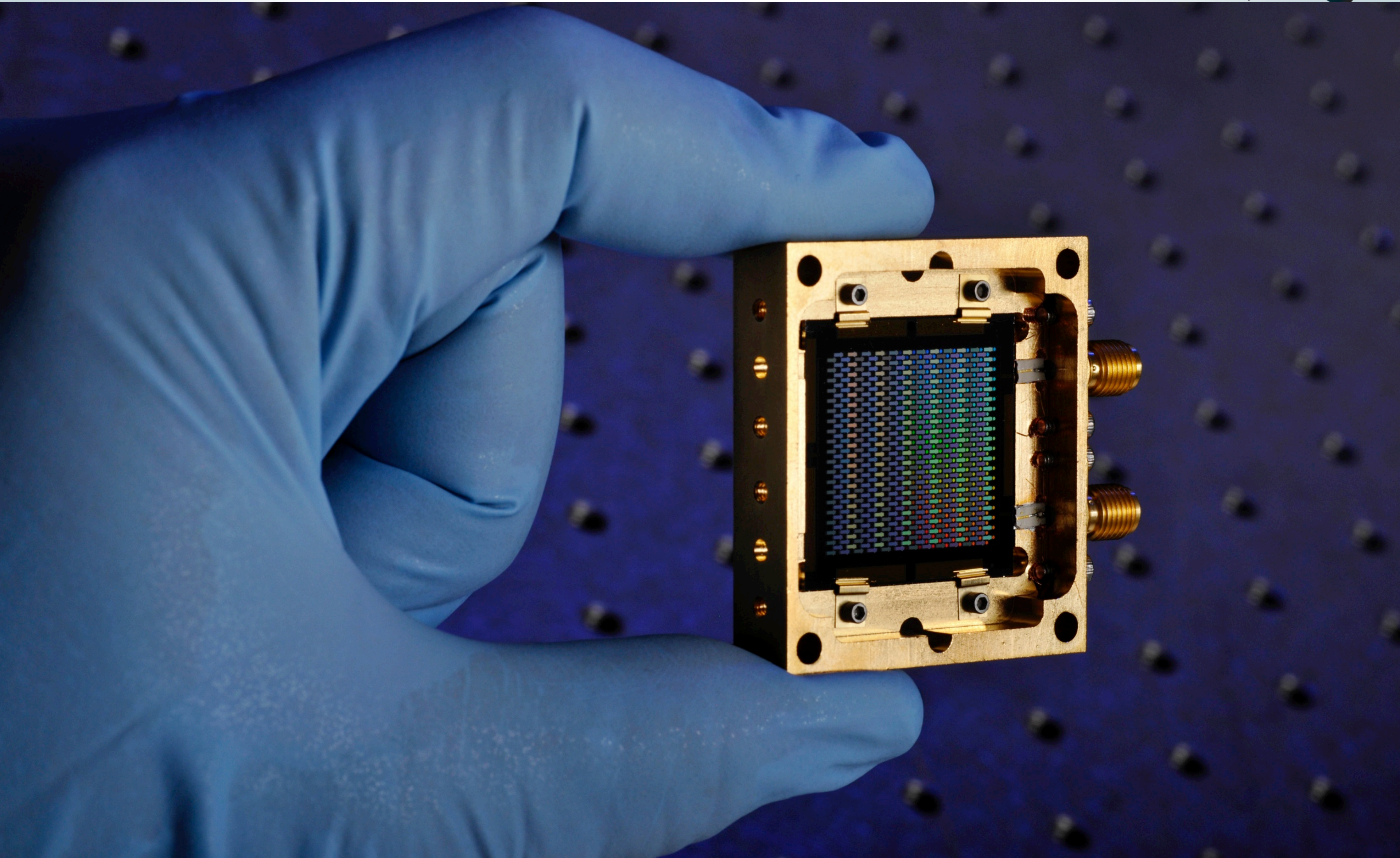

TiN 2G: Hexagonal Packing

- Developed layout to put absorbers on hexagonal lattice while keeping RF readout on rectangular lattice
  - Hexagonal packing is easier to optically couple to than square packing

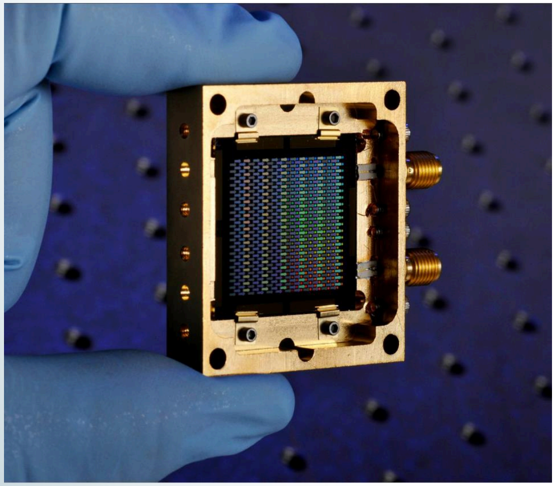

Packaged hexagonally packed TiN 2G devices

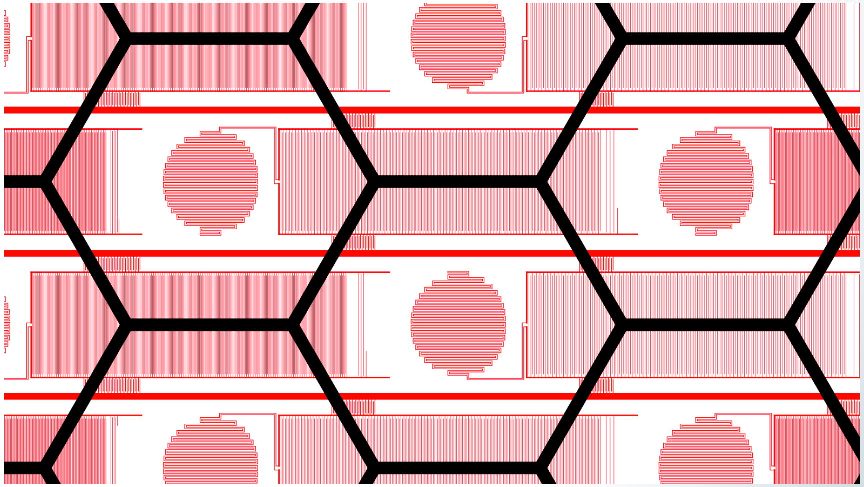

Layout showing inductor, capacitor and coupling (red) + lens positions (black)

TiN 2G: Improving NEP

- Microlens-coupled arrays offer a number of benefits
  - Smaller inductor volume -> increased responsivity
  - Larger capacitor area -> reduced noise
  - Equal capacitor and inductor areas minimizes readout frequency for fixed total pixel area

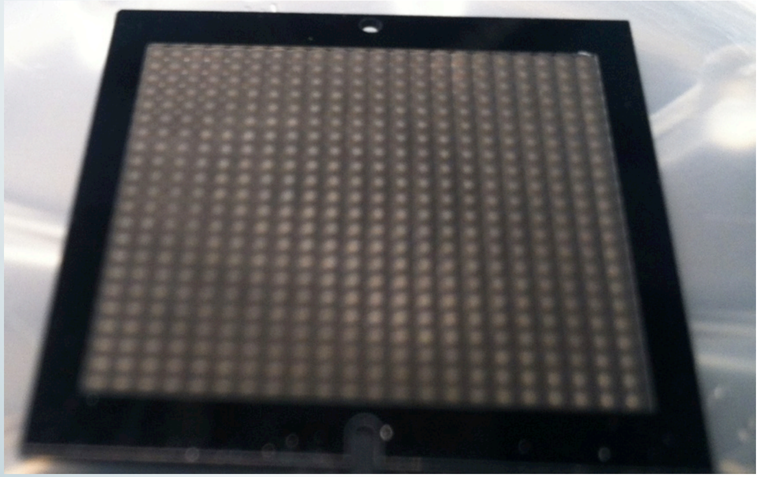

Laser etched square packed lens array

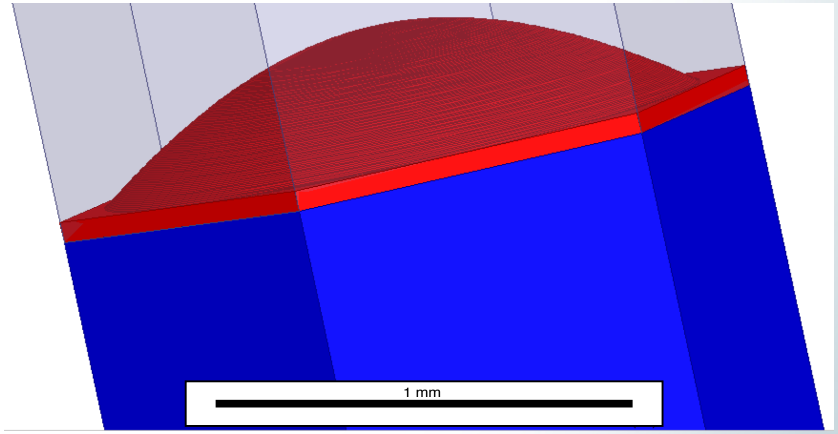

HFSS microlens schematic

Microlens Array Options

- Demonstrated several fabrication methods:
  - Laser etching (Commercial, few $/lens)
  - Photoresist defining and etching
    - In Development - JPL
  - Gradient Lenses (Caltech/JPL ~ $0.20/lens)

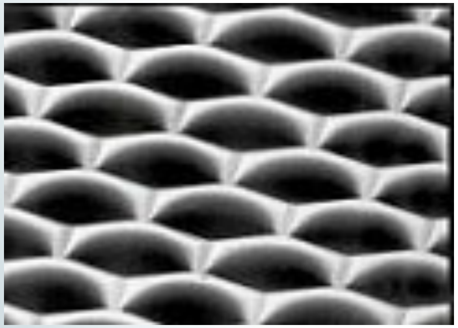

Laser etch lens
(Veld Laser)

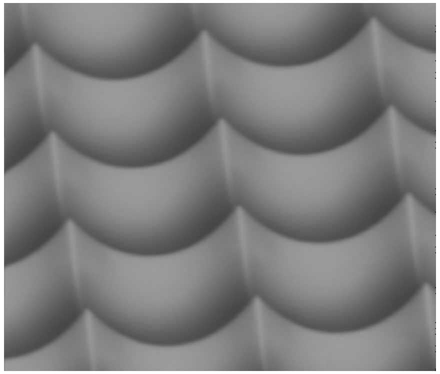

Photo-resist etch
(C. Lee, JPL)

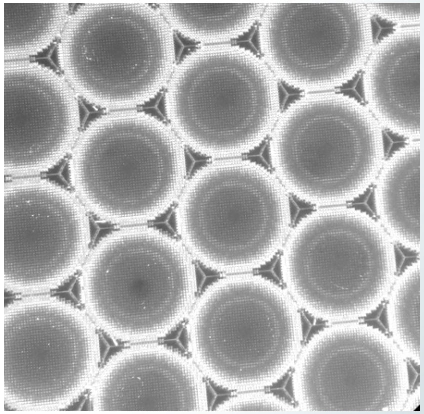

Gradient Lenses
(Caltech/JPL)

Photos of fabricated microlens arrays

Gradient Index (GRIN) Microlens

- Potential low cost lens solution in development at Caltech/JPL
- Made by etching SOI surface to create a gradient in surface index and equal optical path length to focus

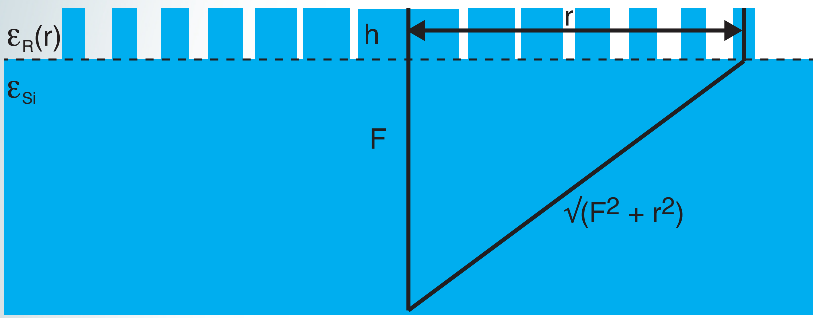

Schematic of etched SOI wafer

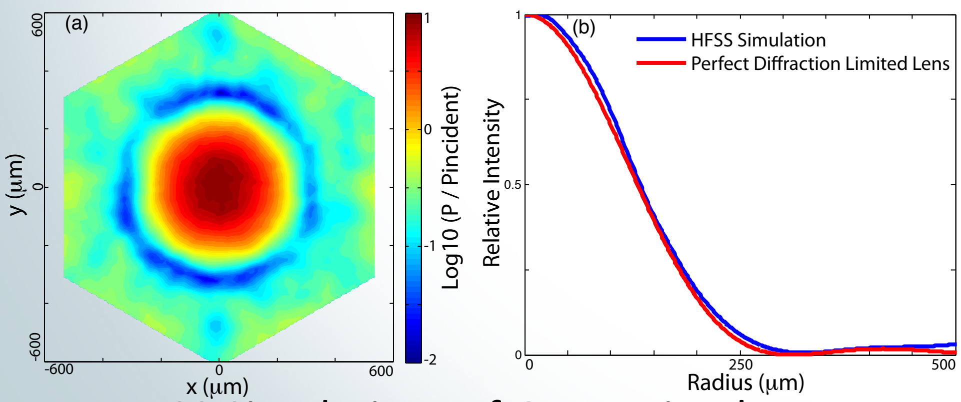

HFSS Simulations of GRIN Microlens

Initial lab measurements - GRIN coupled

Unlensed and **Lensed**

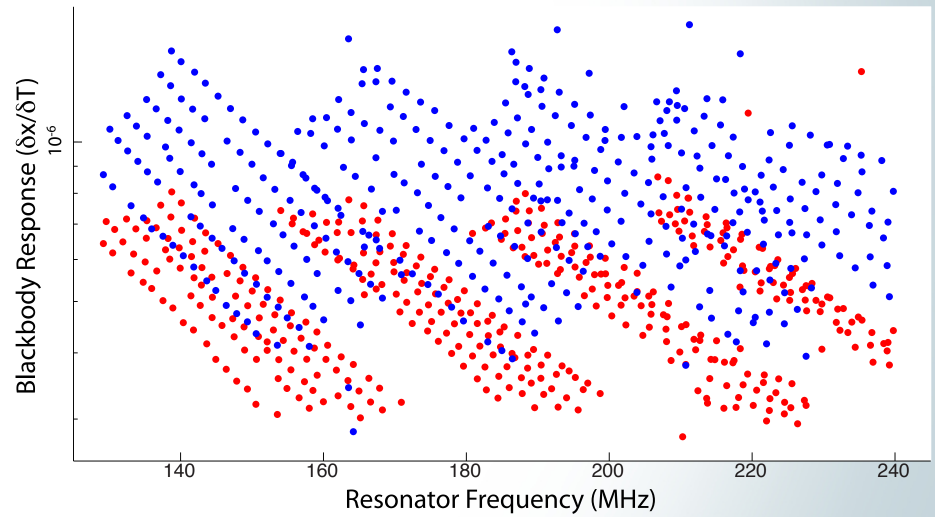

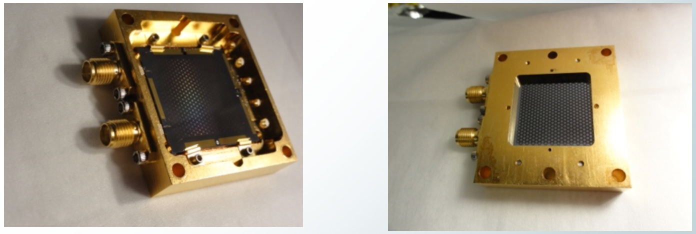

Packaged TiN 2G Test Device

TiN 2G: Initial Lab Results

- 300 K blackbody vs Dark
  - noise significantly higher when viewing 300 K blackbody

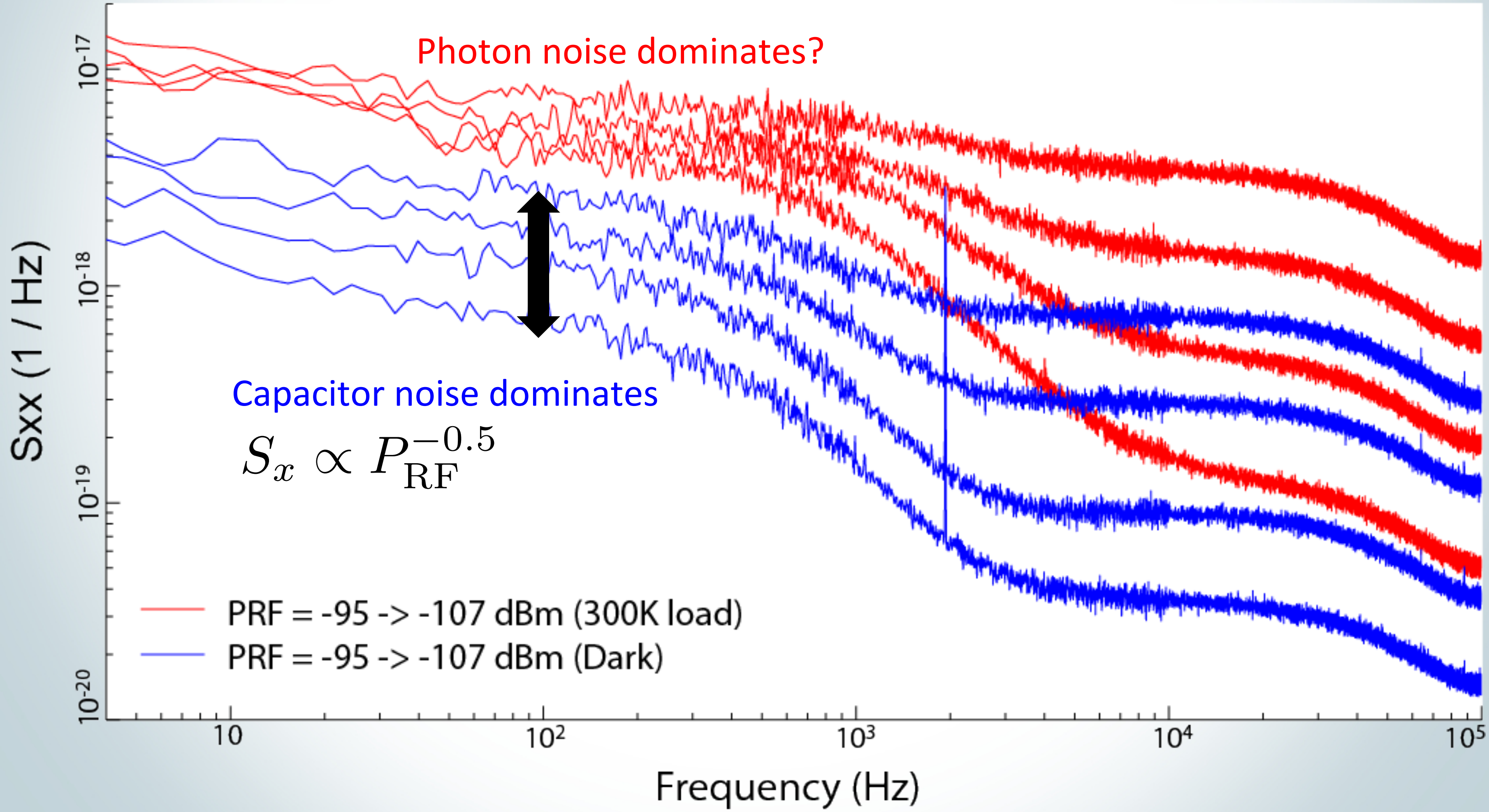

TiN 3G: Dual Pol Design

- Device layout similar to 2G
- Capacitor fingers spread out more
  - Reduce capacitor noise
- Dual polarization layout
  - HFSS simulations show >95% absorption in both polarizations

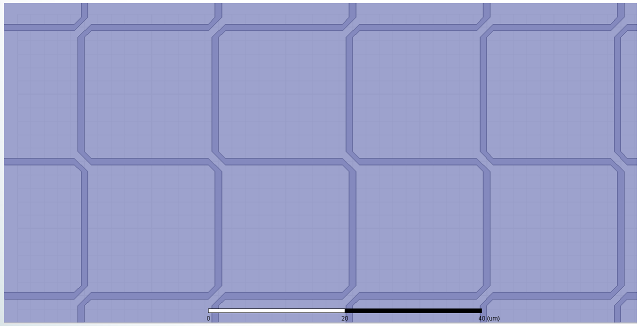

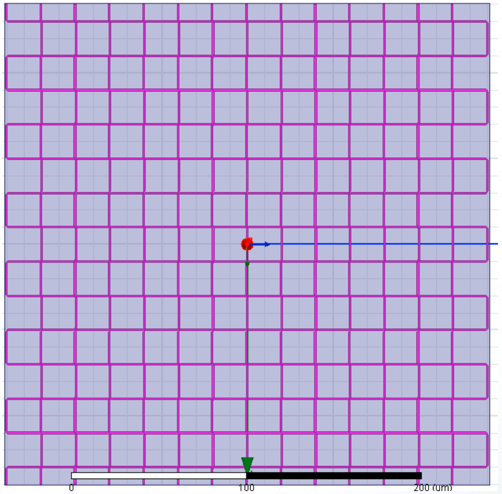

Schematic of a dual polarization sensitive layout

Array Design Details

Ver	Layout	Opt. Couple	Inductor				Capacitor		Freq	Lith Steps	Pixels	Pol.
			Area	Trace	Sep	t	Area	Sep				
			mm^2	μm	μm	nm	mm^2	μm	MHz			
1G	Square	Bare	0.64	4	8	50	<0.4	2	170-240	3	432	1
2G	Hex $1mm^2$	μLens (F/2)	0.3	2	4	50	0.6	2-6	200-240	2	488	1
3G	Hex $1mm^2$	μLens (F/2)	0.3	1	9	100	0.6	4-9	100-150	2	488	2

- 1G: Tested at CSO (MAKO)
- 2G: Currently lab testing
- 3G: Design phase

Summary

- On-sky, full system demonstration of absorber-coupled TiN MKID array
  - > 400 pixels demonstrated on sky
  - Existing FPGA firmware capable of 4k pixels / ROACH
- On-sky NEFD consistent with lab results
  - Reasonable understanding of TiN / pixel design
  - Lens-coupled devices are approaching BLIP
  - Dual-polarization pixel design under way
- Second MAKO/CSO run being planned for spring 2014

- MAKO collaboration: L. Swenson, C. D. Dowell, A. Kovacs, R. Monroe, M. Hollister, H. G. Leduc, J. Zmuidzinas

How do we get a 3D view of the submm sky ?

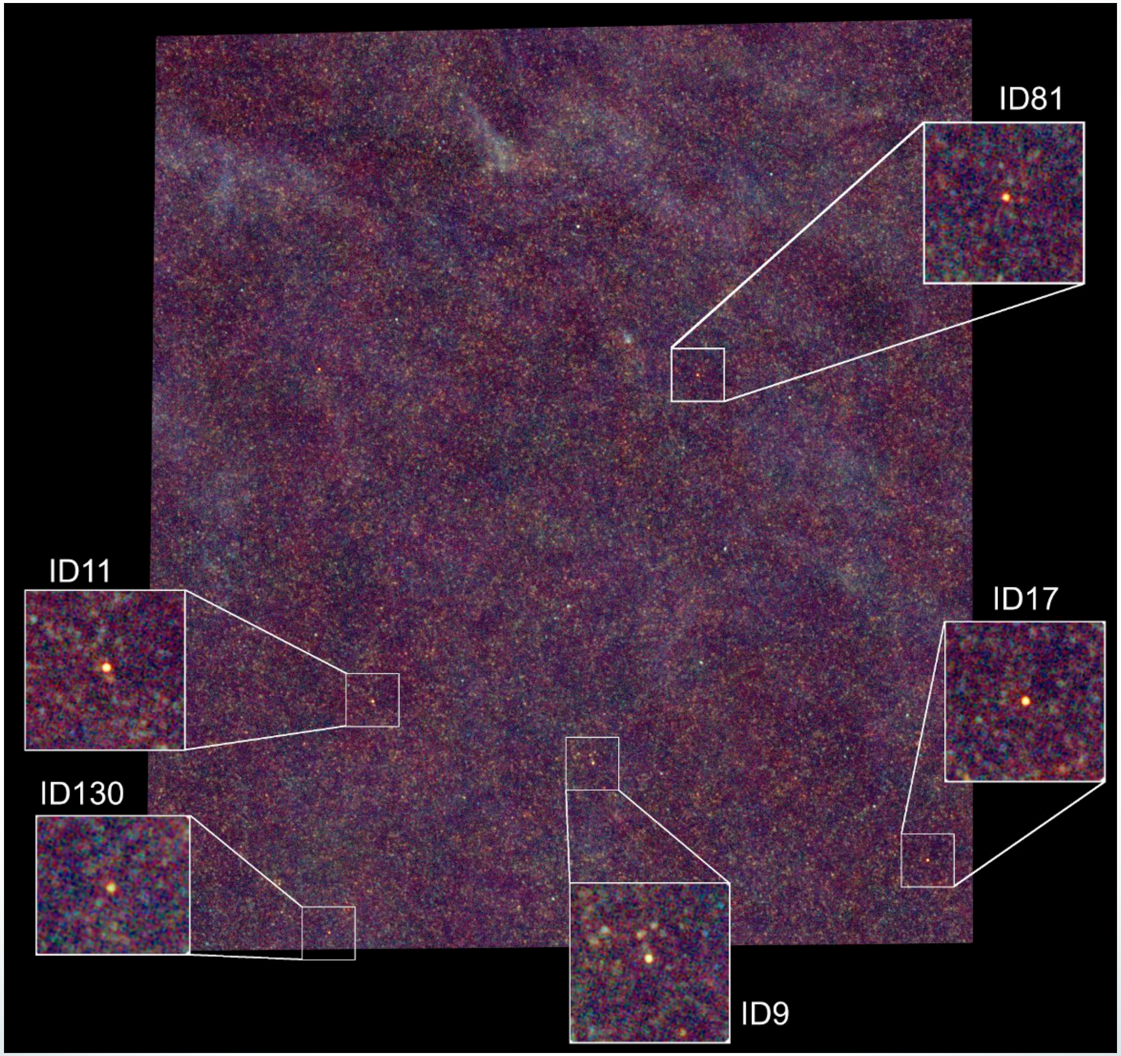

Evolution of the Z-spec concept

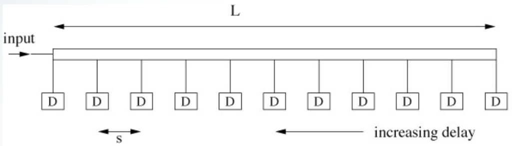

1998: Tapped delay line correlation spectrometer

Thermal noise and correlations in photon detection

1 September 2003 / Vol. 42, No. 25 / APPLIED OPTICS 4989

Jonas Zmuidzinas

CALIFORNIA INSTITUTE OF TECHNOLOGY

Division of Physics, Mathematics, and Astronomy

PROPOSAL TO
YALE UNIVERSITY

For

Development of Superconducting Planar Filterbanks

A subcontract of the proposal entitled:

Photon–counting direct detector arrays for submillimeter imaging and spectroscopy

Submitted by Yale University to NASA (99–OSS-01-SPA)
Prof. R. Schoelkopf, Principal Investigator

1 October 1999 - 30 September 2002

1999: proposal with R. Schoelkopf

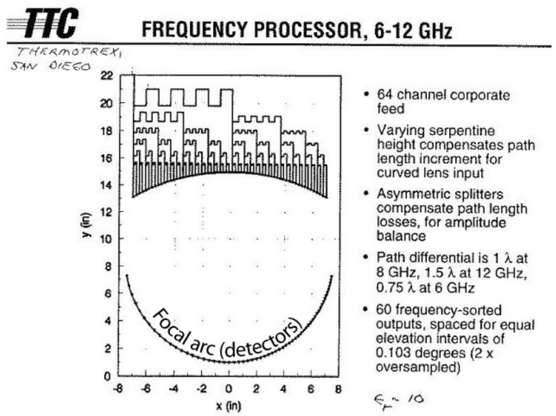

"Pizza" spectrometer: John Lovberg (Sandy Weinreb)
Based on 1971 patent
Superconducting mm-wave version ? (GSFC μSPEC)

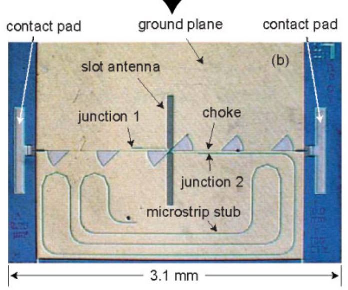

1999: Superconducting microstrip loss test chip

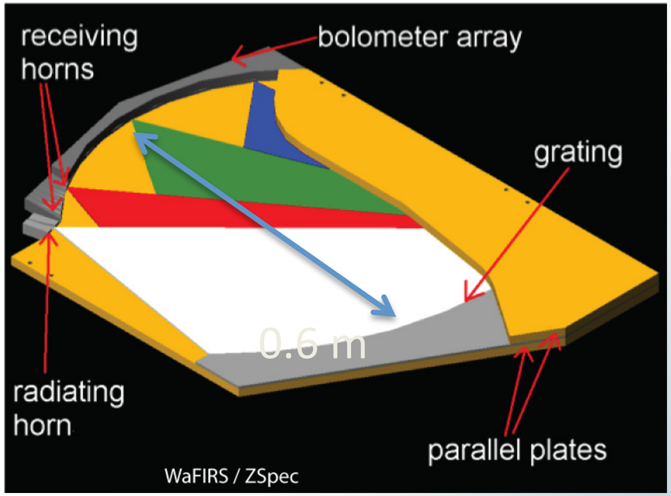

Superconducting mm-wave spectrometer, revisited

(G. Rebeiz: cochlea-inspired channelizing filter)

input

termination

detector

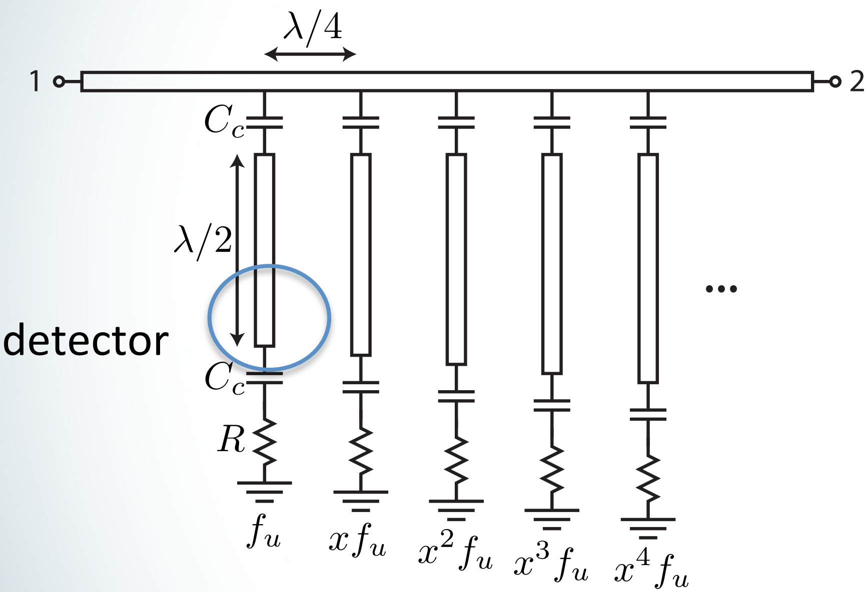

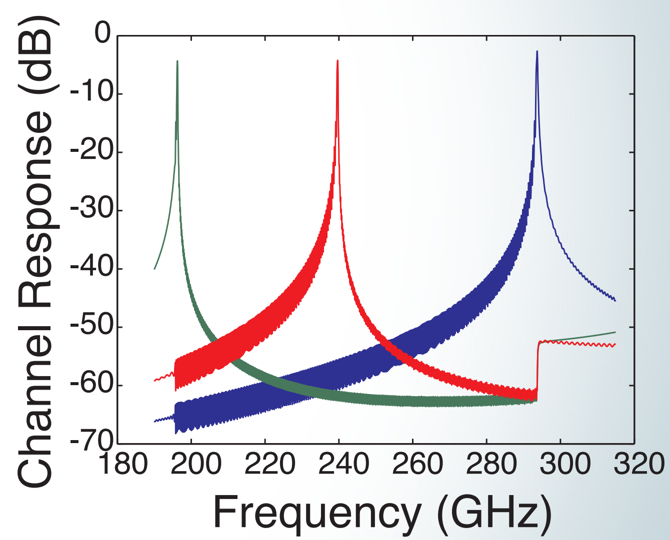

$$A_{\text{total}} < 1\ \text{cm}^2 \text{ for } R = 700,\ \lambda = 1\ \text{mm}$$

See Shirokoff et al, Proc. SPIE, 2012

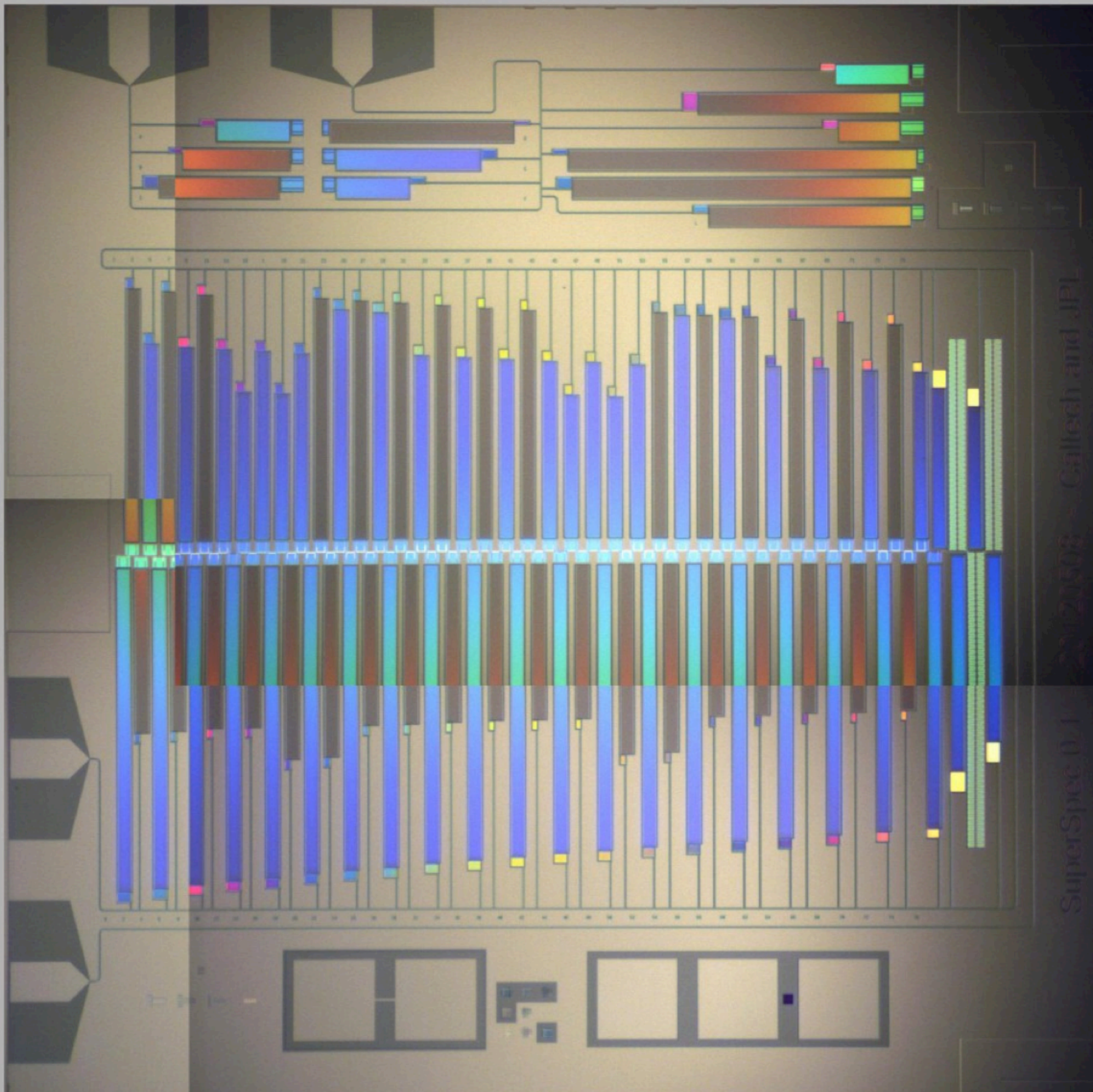

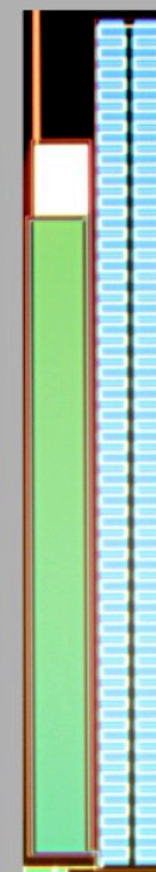

Superconducting spectrometer

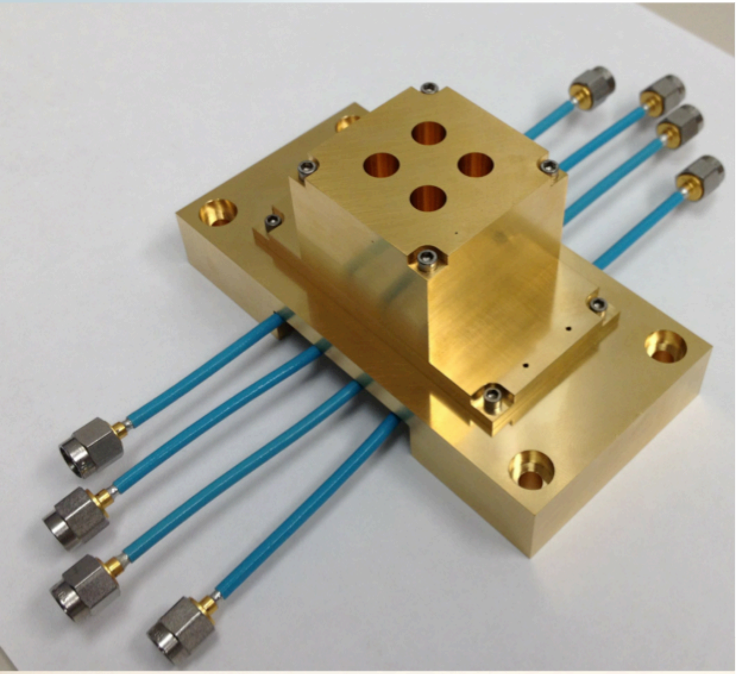

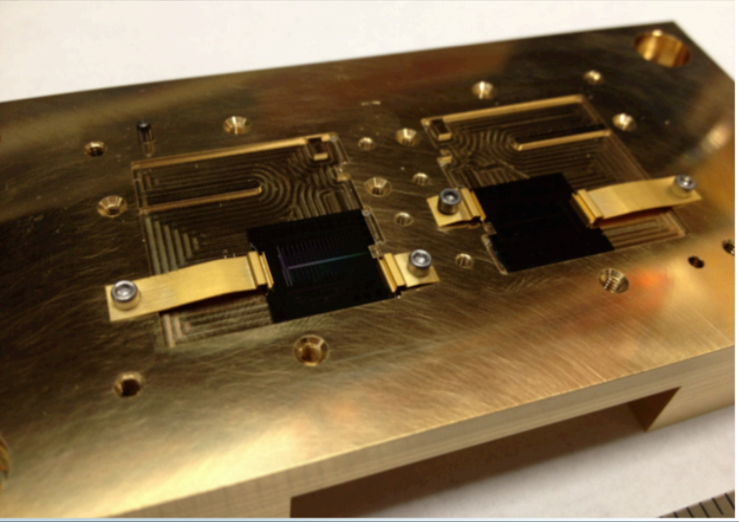

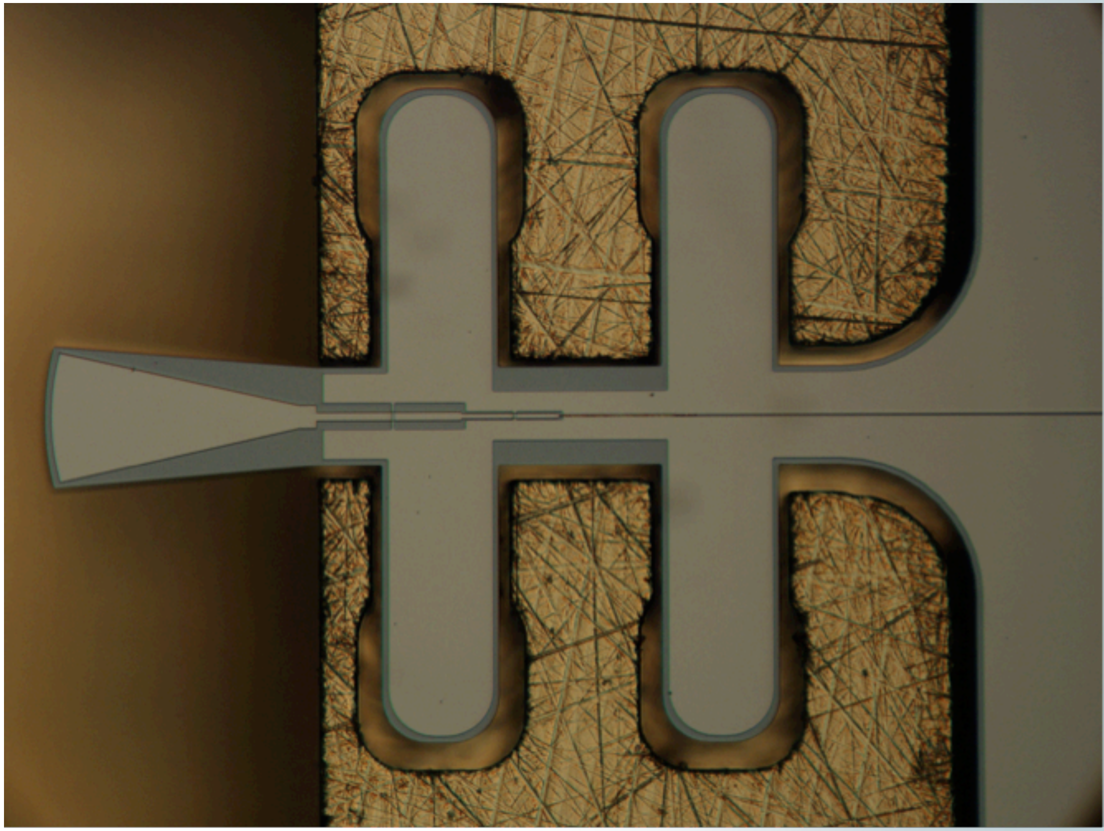

Bibliography

- Zmuidzinas J. "Superconducting Microresonators: Physics and Applications", Annu. Rev. Condens. Matter Phys. 2012 **3**:169-214 (2012)
- Barends R., et al. "Quasiparticle Relaxation in Optically Excited High-Q Superconducting Resonators", Phys. Rev. Lett. **100**:257002 (2008)
- Doyle S, et al. "Lumped element Kinetic Inductance Detectors", J. Low Temp. Phys. **151** 530-36 (2008)
- Noroozian O, et al., "Crosstalk Reduction for Superconducting Microwave Resonator Arrays", IEEE Trans. Micr. Theory Tech. **60** 1235-1243 (2012)
- Swenson L., et al. "Operation of a titanium nitride superconducting microresonator detector in the nonlinear regime", J. Appl Phys. **113** 104501 (2013)
- McKenney C, et al. "Design considerations for a background limited 350 micron pixel array using lumped element superconducting microresonators", Proc. of SPIE **8452** 84520S (2012)
- Swenson L, et al. "MAKO: A pathfinder instrument for on-sky demonstration of low cost 350 micron imaging arrays", Proc. SPIE **8452** (2012)
- Swenson L, et al. "The Status of MAKO", Proceedings of LTD-15 (2013)
- McKenney C, et al. "Lumped element kinetic inductance detectors: Pixel design for large scale far infrared arrays", Proceedings of LTD-15 (2013)

CCAT

BACKUP SLIDES

SHARC-II Optics

SHARC II: a Caltech Submillimeter Observatory facility camera with 384 pixels

C. Darren Dowell[a], Christine A. Allen[b], Sachidananda Babu[b], Minoru M. Freund[b], Matthew B. Gardner[a], Jeffrey Groseth[a], Murzy Jhabvala[b], Attila Kovacs[a], Dariusz C. Lis[a], S. Harvey Moseley, Jr.[b], Thomas G. Phillips[a], Robert Silverberg[b], George Voellmer[b], and Hiroshige Yoshida[c]

[a]California Institute of Technology, Mail Code 320-47, 1200 E. California, Pasadena, CA 91125
[b]NASA-Goddard Space Flight Center, Greenbelt, MD 20771
[c]Caltech Submillimeter Observatory, 111 Nowelo St., Hilo, HI 96720

Table 2. Summary of SHARC II Optics.

Parameter/Item	Value/Composition
f/ ratio	f/4.5
pixel size	$4.6'' \times 4.6''$
field of view	2.3 square arcminutes
angular resolution, 350 μm	$9''$ FWHM
mean Strehl ratio, 350 μm	0.95
window	1 mm high-density polyethylene
77 K filter	z-cut crystal quartz, 2 mm front surface: 58 μm clear polyethylene back surface: 50 μm black poly, 8 μm clear poly
4 K filters	quartz (same specifications) 33 cm^{-1} lowpass (Cochise Instruments/P. Ade)
4 K bandpass filters (Cochise Instruments/P. Ade)	350 μm, $\Delta\lambda(\mathrm{FWHM})/\lambda = 0.13$ 450 μm, $\Delta\lambda(\mathrm{FWHM})/\lambda = 0.10$ 850 μm, $\Delta\lambda(\mathrm{FWHM})/\lambda = 0.08$

MAKO Optics

Optics designed to match SHARC-II as much as possible

Parameter/Item	Value/Composition
f/ratio	f/4.5
pixel size (geometric)	0.8 μm x 1.4 μm (0.8 μm x 0.8 μm absorber)
pixel size (on sky)	3.59″ x 6.57″ (3.59″ x ~3.59″ absorber)
filling factor	57%
rows x columns (# pixels)	16 x 27 (432)
usable pixels	418 resonances identified, >380 currently used (88-97% yield)
field of view	105″ x 97″ (2.83 square arcminute)
angular resolution, 350 μm	9″ (?)
mean Strehl ratio, 350 μm	0.95 (?)
window	1 mm high-density polyethylene
65 K stage	z-cut crystal quartz, 2 mm front surface: 58 μm clear polyethylene back surface: 50 μm black poly, 8 μm clear poly
4 K	100 μm and 300 μm low-pass filter (QMC)
250-270 mK (on sample holder)	350 μm bandpass, 10% bandwidth (QMC)

TABLE I: Summary of MAKO optics

Single-channel analog readout

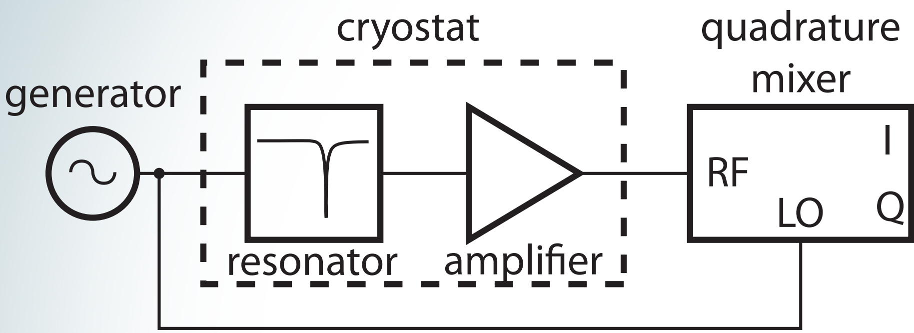

$I \propto \mathrm{Re}(S_{21})$

$Q \propto \mathrm{Im}(S_{21})$

$$\begin{bmatrix} \delta A \\ \delta B \end{bmatrix} = \begin{bmatrix} \cos\theta & \sin\theta \\ -\sin\theta & \cos\theta \end{bmatrix} \begin{bmatrix} \delta I \\ \delta Q \end{bmatrix}$$

$$\delta x(t) \propto \delta A(t)$$
$$\delta Q_i^{-1}(t) \propto \delta B(t)$$

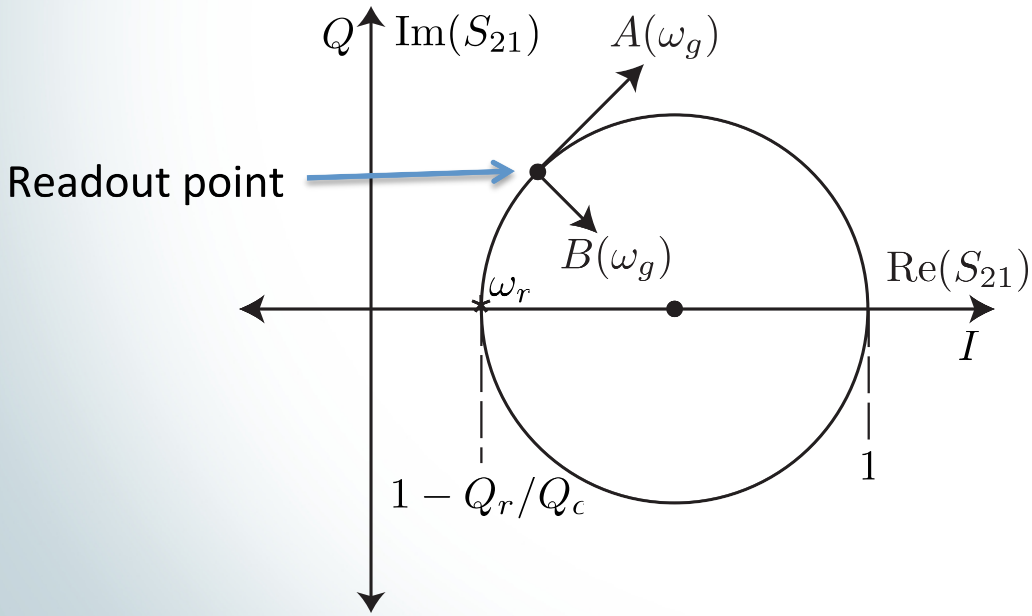

Resonator frequency, Q monitored at ~100 kHz sampling rate

Response bandwidth set by quasiparticle lifetime and resonator ring-down time